The establishment of endosymbiosis: An experimental and computational investigation using the artificial symbiont *Synechocystis*

Megan Elisabeth Stig Sørensen

MSc by research

University of York

Biology

June 2015

Abstract

Ancient evolutionary events are difficult to study because their current products are derived forms altered by millions of years of adaptation, which obscures how these key transitions occurred. The primary endosymbiotic event formed the first photosynthetic eukaryote; this radiated to become plants and algae, and has therefore had vast consequences for life on earth. Modelling, if grounded correctly with biology, enables events such as this that cannot directly be studied, to be inferred by building analogous simulations. This project applies metabolic modelling, using flux balance analysis (FBA), to this evolutionary transition to study the metabolic adaptations necessary for the symbiont to transition from free-living to endosymbiotic.

The model was validated for the bacterial symbiont in isolation by testing the biomass composition, the nutrient limitation predictions, and the predictions for growth rates and metabolic fluxes in different environmental conditions. Subsequently the model was applied to a symbiotic state. Within the symbiotic state, a carbon compensation cost was used to manipulate the behaviour of the symbiont and therefore made it possible to compare the metabolism between a 'selfish' and a cooperative symbiont. These behaviour types are analogous to the expected difference between a newly established endosymbiosis that is governed by conflict and a well-developed one that has reached a mutual-benefit state. This project was able to develop predictions for these key states within the endosymbiotic context. Overall, the results show the applicability of FBA modelling to those ancient evolutionary transitions that were driven by metabolic exchanges, like endosymbioses.

Contents

List of Figures:

List of Tables:

List of Accompanying Material:

iHK677_standard.xls

The model of free-living Synechocystis

iHK677_symbiotic.xls

The model of symbiotic Synechocystis, includes all the different exchange reactions examined

mas.java

Part of the code to implement the model

FBAreader.java

Part of the code to implement the model

fba.java

Part of the code to implement the model

Acknowledgments:

I would like to thank first and foremost my supervisors Michael Brockhurst and A. Jamie Wood for making this project possible and extremely enjoyable, and for all their analytical guidance. I would also like to thank Ewan Minter for his help and for taking the time to teach me many of the lab techniques. I would like to thank the larger research group that I am part of, which, in addition to those named above, includes Duncan Cameron, Andrew Dean, Chris Lowe and Richard Law. It had been a great project to be involved in and I look forward to the work to come.

In addition I would also like to thank my TAP panel, Jon Pitchford and Julia Ferrari, for their suggestions and interesting discussions, and the whole of the L0 Brockhurst lab group for the helpful suggestions during the lab meetings and during general conversations.

Author's Declaration:

I, Megan Elisabeth Stig Sørensen, declare that all the material contained within this thesis except for the work outlined below is a result of my own work and has been written solely by myself.

The initial re-creation of the Knoop model was done by A. Jamie Wood. This involved writing the scripts that carried out the FBA modelling based on standard practise. We then both worked on the modifications to get it working correctly.

The mass spectrometry work was done in collaboration with Duncan Cameron and Mike Burrell at the University of Sheffield. Along with Mike Burrell I prepared the samples for analysis and collected the data. The data was formatted into the required data files by Mike Burrell and Duncan Cameron, and they carried out the PCA and OPLS analysis. All further analysis, including the identification of masses, was performed by myself.

Introduction:

Endosymbiosis has led to some of the most important transitions in the evolution of eukaryotes, including their origin and later the formation of photosynthetic eukaryotes (Keeling *et al.*, 2013). The endosymbiotic origin of organelles was a controversial concept, but championed by Lynn Margulis (Sagan, 1967) it was eventually accepted with the advent of molecular techniques (Bonen & Doolittle, 1975; Schwarz & Kössel, 1980). Endosymbiosis, a symbiotic relationship where one organism resides within another, is a common occurrence in algae, though the transition to organelles is rare (Cavalier-Smith *et al.*, 2013). The primary endosymbiosis event involved the uptake of a cyanobacterium to form the first photosynthetic eukaryote; this has since radiated to become the land plants and algae. The symbiont has experienced hundreds of millions of years of coevolution and genome reduction to the extent that it has lost autonomy and become an organelle – the chloroplast (Dyall *et al.*, 2004). This very derived form makes the establishment of this major endosymbiotic event difficult to study.

Endosymbiotic relationships occur in a diverse range of organisms and have many advantages, such as protection from predation (Tsuchida *et al.*, 2010), increased photoprotection (Hörtnagl *et al.*, 2007) and the provision of luminescence (Tebo *et al.*, 1979). At the core of the interaction, however, is nutrient exchange. For example, aphids and their obligate endosymbiont, *Buchnera aphidicola*, share the synthesis of essential amino acids to the extent that within one pathway some enzymes will be produced by the host and others by the symbiont (Wilson *et al*., 2010). Furthermore, Vigneron *et al.* (2014) demonstrated that aposymbiotic cereal weevils could only grow on starch if it was complemented with tyrosine and phenylalanine, which their endosymbiont normally provides.

This is particularly salient in photosymbiosis where one organism can provide carbon through the photosynthate and in return receives nitrogen and other minerals/vitamins. This exchange is seen across a range of organisms: cyanobacteria and fungi in types of lichen (Honegger *et al.*, 1991), land plants and arbuscular mycorrhizal fungi (Pfeffer *et al.*, 1999), and dinoflagellates and coral (Yellowlees *et al.,* 2008). Its universal nature makes it a likely candidate for the initial and primary benefit of photosymbiosis.

Following the singular event of the primary endosymbiosis, subsequent secondary endosymbioses have arisen and are far more common. These occur when a eukaryote engulfs another photosynthetic eukaryote. These events do not necessary fixate and current research is revealing the prolific nature of transient facultative endosymbioses in algae. The partnership in this case is therefore more fluid; with the dependency increasing under some conditions, mostly when nutrient-poor, and decreasing under others, normally when nutrient-rich (Johnson, 2011; Muscatine & Porter, 1977).

Paramecium and *Chlorella* Endosymbiosis

An example of an endosymbiosis on the borderline between facultative and obligatory is that between the ciliate host *Paramecium bursaria* and the green algae *Chlorella* spp.. The symbiont is vertically inherited and the two cell cycles are synchronised (Kodama *et al.*, 2012), which indicates a very stable relationship. However, as both organisms can survive if isolated, it remains a facultative symbiosis. *Paramecium* and *Chlorella* have a classical photosymbiotic exchange, whereby the *Chlorella* provides organic carbon fixed by photosynthesis and *Paramecium* in return supplies organic nitrogen. It is estimated that the *Chlorella* endosymbionts release 57 % of their fixed carbon to their host (Johnson 2011), primarily as maltose (Ziesenisz *et al.,* 1981). Ziesenisz *et al.* demonstrated that maltose was provided both day and night but by two different pathways: in the light maltose is synthesised *de novo* from the products of the Calvin Cycle while in the dark it is formed from starch degradation. In stable partnerships such as this the exchange is not a passive process, for instance host Ca^{2+} inhibits serine uptake into *Chlorella* and glucose increases the uptake (Kato *et al.*, 2008a and 2008b). If the symbiont's maltose is broken down to glucose by the host, then the control process would facilitate a reward system for co-operative symbionts.

The nitrogen source is not yet verified, though there are several suggestions. The Japanese strain F36-ZK has lost its nitrate reductase activity but can utilise amino acids, therefore these have been proposed to be the source (Kato *et al.*, 2008b). Alternatively, other work suggests that *Paramecium* produces nitrogen waste in the form of nucleic acid derivatives, such as guanine and xanthine (Soldo *et al.,* 1978), which are then assimilated by *Chlorella* (Shah *et al.,* 1984). Nucleoside recycling has been demonstrated in other endosymbioses (Ramsey *et al.*, 2010), and the efficiency of using a host waste product would decrease the cost of symbiosis. Additionally, there are mixed results for ammonia utilisation, with some studies supporting it as a candidate

source (Albers *et al.*, 1982) and others finding poor *Chlorella* growth on ammonia (Kato *et al.*, 2006), which may be due to strain specific adaptations or unknown assimilation pathways.

This partnership has been studied thoroughly due to the ease of isolation and reinfection, which have been documented by Kodama *et al.* (2011). The two organisms are interdependent to the extent that their circadian cycles are linked. For instance, it has been demonstrated that *P. bursaria* with *Chlorella* have a longer period than aposymbiont ones, arrhythmic *P. bursaria* mutants can be rescued by symbionts, and if the host and symbiont are in different phases *P. bursaria* will gradually shift to the match *Chlorella's* (Miwa *et al.*, 1996). This relationship is very stable and is the product of thousands of years of co-evolution; it is therefore an excellent model to study pre-existing endosymbioses.

Environmental conditions, such as light and nutrients, can shift a symbiosis across the parasitism–mutualism continuum. Photosymbioses are heavily influenced by light because the symbionts only lead to a net benefit above a light intensity threshold (Dean *et al.*, in prep). In the establishment phase the relationships are particularly susceptible; for a stable relationship to arise light levels above the cost-threshold are necessary. If kept in darkness, the cost of symbionts can lead to their complete loss. For instance extensive dark treatments can remove *Chlorella* from *P. bursaria* (Kodama *et al.*, 2011).

There is one example of a second primary endosymbiont event. The amebae *Paulinella chromatophora* has been found to have an organelle-like structure, a chromatophore, which is derived from a cyanobacterium – *Synechococcus* (Marin *et al.*, 2005*)*. There have been several, possibly 32, genes transferred to the nucleus (Nowack *et al.*, 2011), and these genes are biased towards a role in photosynthesis, for instance psaE which is a peripheral protein in photosystem I. This suggests that these transfers are examples of fully functional endosymbiotic gene transfers and since some of the proteins encoded are localised to the chromatophore, a protein import mechanism is implicated. There are several suggested mechanisms of protein import but its exact nature is currently unknown (Body *et al.*, 2009). Relative to the primary endosymbiotic event this is a 'recent' event, but it is still ancient, occurring approximately 60 million years ago

(Mackiewicz *et al.*, 2012). It highlights the propensity for cyanobacteria and protists to form endosymbioses that can in rare instances evolve to become an organelle.

Such pre-existing endosymbioses cannot be used to study the origin of endosymbiosis. The organisms have co-evolved together and so even re-infection has very little bearing on the actual initiation process. In order to study the establishment of endosymbiosis, an entirely novel partnership is required to ensure that no adaptation has occurred. To model the primary endosymbiotic event an artificial endosymbiosis between a cyanobacterium and a protist is the most suitable. There is not much known about the host in the primary endosymbiotic event other than it was a unicellular eukaryote that was heterotrophic and capable of ingesting bacteria.

Recently an artificial endosymbiosis was created by Ohkawa *et al.* (2011) by supplying aposymbiotic *Paramecium bursaria* with Synechocystis PCC6803. These organisms do not naturally form a symbiosis and so have not co-evolved. *Synechocystis* is a cyanobacterium that cannot fix nitrogen and therefore is capable of acting as a photosymbiont. The metabolic exchange is unlikely to be identical to that between *P. bursaria* and *Chlorella* because the maltose exporter is an Archaeplastida innovation and there is no evidence to suggest *Synechocystis* can produce maltose (Ball *et al.*, 2011; Niittylä *et al.*, 2004). The exchanges, however, are probably similar because *Paramecium's* recognition of potential symbionts will most likely require a supply of certain metabolites. Therefore, the knowledge of the natural symbiosis can help to direct the investigation. Furthermore, *Synechocystis* shares a common ancestor with the cyanobacteria-like symbiont that was engulfed in the primary endosymbiont event. This therefore is a suitable model to understand the establishment, and not merely the result, of endosymbioses, and to make inferences about the primary endosymbiotic event.

Metabolic Modelling

In order to understand the evolution of endosymbiosis it is crucial to know the metabolic exchanges, and this can be achieved through metabolic modelling. A powerful theoretical method for analysing metabolism is Flux Balance Analysis (FBA) modelling, which is capable of predicting the optimal metabolic fluxes of an organism and thus its growth rate (Orth *et al.*, 2010; Varma & Palsson, 1994a and 1994b). Within the constraints of stoichiometry, FBA calculates the flux through each known reaction in the cell. The flux values are optimised with respect to the objective function. This

varies, but is commonly biomass on the assumption that organisms 'prioritise' growth and division. The model requires a large amount of data and so is limited to organisms with in-depth metabolic and genomic information. Furthermore, the enzymes and genes are considered to be Boolean values (they are 'on' or 'off'), therefore there is no regulation, and it assumes no underlying constraints prevent optimality. Despite being a simplification, FBA has great potential. It has shown to be applicable to biotechnology (Milne *et al.*, 2009) and in several cases successfully predicted the outcome of evolution experiments (Harcombe *et al.*, 2013; Ibarra *et al.*, 2002). The assumption of optimality means that quantitatively its predictions are often biologically too high and even sometimes unachieved (Fischer *et al.*, 2005), but it has been shown to have good qualitative predictions.

There have been previous applications of FBA to symbiotic organisms. These have been based on very stable symbioses and have modified the objective function to include the metabolic exchange. For instance, Resendis-Antonio *et al.* (2007) created an FBA model for *Rhizobium etti,* which provides ammonia to legumes. The objective function is entirely based on the exchange which is plausible as the bacterium's reproductive stage is separate to its symbiotic stage, rendering the bacterial biomass unnecessary. This model was used to predict the effect of gene knockouts, and these predictions have fairly high congruence to experimental data. Furthermore, Thomas *et al.* (2009) modelled the endosymbiont *Buchnera aphidicola* and used knockout analysis to show an unusually high level of gene essentiality (84%), which is the expected result of dramatic genome reduction that often accompanies stable endosymbionts. These examples demonstrate that FBA is a valid approach for modelling metabolism in symbioses. The use of the exchange reaction as the objective function is valid in these cases; however, it would not be appropriate in the *Paramecium*-*Synechocystis* relationship. This is because it is novel relationship and the model will be used to study the transition from a free-living state to a symbiotic one. This means that the bacterial biomass cannot be dismissed because it will be growing simultaneously to the metabolic exchange.

Several FBA models have been created for *Synechocystis* PCC6803, which is a very well characterised organism. The first FBA model for *Synechocystis* was created by Morgan *et al.* (2005) they included a glyoxylate shunt and based their objective function on experimentally measured proportions of the major cellular components. This was

later elaborated by Nogales *et al.* (2012) who kept the earlier proportions but split the components into a detailed compound level. The detailed components were estimated by bioinformatics and no additional experimental validation was added. This elaborated objective function is the same as that used in the latest FBA reconstruction by Knoop *et al.* (2013). This model has 759 reactions, based on 677 genes. It includes a background ATP maintenance amount, the formation of reactive oxygen species from the light, sets a basal level of respiration in the light, and sets the proportion of photorespiration (3%). It assumes that light is the limiting factor and nutrients are unbounded. It does not include either the glyoxylate shunt or the OGDH complex, which can allow a complete TCA cycle but rather predicts an incomplete TCA cycle in the light, and in the dark a unique cyanobacteria bypass is used. The bypass, proposed by Zhang *et al*. (2011), involves two alternative enzymes which together convert 2-oxoglutarate into succinate. Furthermore, the model was iteratively performed over a series of light intensities with circadian regulation of certain genes to model diurnal variation.

Metabolic modelling can therefore be used to predict the nutrient exchange in this artificial endosymbiosis, using the natural symbiosis as a reference. In this project the most recent FBA model (Knoop *et al*., 2013) was first refined and then benchmarked by testing predictions for free-living *Synechocystis* with experimental data. The model was then modified for a symbiosis setting by introducing an 'exchange reaction' that forced nutrient exchange. *Synechocystis* must therefore export a carbon compound in order to receive any nitrogen. It is an acceptable assumption that the only nitrogen available will be that which the *Paramecium* host provides because this is an *endo*symbiosis meaning that the *Synechocystis* is physically inside the host. Endosymbionts satisfy more of the assumptions of FBA modelling than other organisms because the host provides a very stable environment which can potentially lead to more stable and less fluctuating gene expression. Furthermore, obligate endosymbionts that have co-evolved with their host experience gene reduction and a decrease in transcriptional regulation, both of which makes FBA modelling more appropriate (Thomas *et al.*, 2009). There is unfortunately not yet sufficient data to create a *Paramecium* FBA model owing to its genetic complexity that has prevented any detailed whole genome sequencing.

The exchange can be viewed as a transaction in which the organisms are trading goods. By altering the ratio and parameters values in the exchange reaction different degrees of cooperation/different trading behaviours were explored. *Paramecium* as the "seller" sets

the “price” of the trade, which determines how many molecules of carbon *Synechocystis* must export per molecule of nitrogen it receives. This “price” is dictated by the carbon to nitrogen ratio (C:N) that represents their relative value. The parameter value incorporates the behaviour of the *Synechocystis;* whether it tries to cheat the ‘seller’ or whether it pays the fair cost. This centres on the carbon contained within some of the nitrogen sources that the host exports. If the symbiont is cooperative it pays an extra carbon compensation costs to account for any carbon it receives, but if “selfish” it benefits from this additional carbon. The C:N ratio represents how costly the exchange is for *Synechocystis*, while the compensation value represents the degree of cooperation of the symbiont. The ability to explore different degrees of cooperation provides a means to model different initiation stages of a developing symbiosis rather than just predicting the final outcome.

To understand the establishment of endosymbiosis and therefore its evolution, evidence of the initial metabolic exchange between the host and symbiont is necessary. Through a combination of experimental data and FBA modelling this project hopes to contribute to this required knowledge by studying the synthetic endosymbiosis between *Synechocystis* and *Paramecium*.

Methods:

Modelling

The FBA model was based upon the iHK677 model published by Knoop *et al.* (2013) with modifications by myself and A. Jamie Wood. The predicted growth rates in the two models were identical to 13 decimal places and only one flux rate had more than a 10^{-12} difference. The modifications were mostly to the values of the upper and lower bounds, and the explicit inclusion of transport reactions. The symbiotic exchange reaction was included when appropriate. Biomass was used as the objective function. A second optimisation was applied that minimises the reaction fluxes while maintaining the optimum biomass to select an optimal solution and removes futile cycles.

The only constraints on reaction fluxes were taken from the publication and are: basic ATP consumption (0.13 mmol gDW^{-1} hr^{-1}), a residual respiration rate (0.2263 mmol gDW^{-1} hr^{-1}), Mehler-like reaction (0.2263 mmol gDW^{-1} hr^{-1}), reactive oxygen species production at PSII (0.0477 mmol gDW^{-1} hr^{-1}), and Mehler reaction at PSI (0.0473 mmol gDW^{-1} hr^{-1}). In the standard condition, light is assumed to be the limiting factor and is set to 18.7 mmol gDW^{-1} hr^{-1} and nutrients are considered unlimited, though carbon uptake is restricted to bicarbonate (HCO_3) and nitrogen uptake is as nitrate (NO_3^-). The model includes the reactions for other sources but these have a default value of 'off'. The iHK677 model encompasses 677 genes that encode for 759 reactions. The network defines six cellular compartments - the cytosol, plasma membrane, thylakoid membrane, thylakoid lumen, carboxysomes, and periplasm - in addition to the extracellular space.

Extra reactions were required for guanine metabolism because the genes have not been identified in *Synechocystis*. A standard active transport reaction was added (reaction 1) and a typical bacterial catabolism reaction that encompasses the several stages of guanine degradation (reaction 2) (Nygaard *et al.*, 2000).

Reaction 1: $ATP_{[cyt]} + H_2O_{[cyt]} + Guanine_{[ext]} \longleftrightarrow Guanine_{[cyt]} + ADP_{[cyt]} + Orthophosphate_{[cyt]}$

Reaction 2: $Guanine_{[cyt]} + 6*H_2O_{[cyt]} + 2*O_{2[cyt]} \longleftrightarrow 2*Urea_{[cyt]} + CO_{2[cyt]} + 2*H_2O_{2[cyt]} + NH_{3[cyt]} + Glyoxylate_{[cyt]}$

For the nutrient limitation analysis the concentration ranges for nutrients were based of the Redfield ratio (106C : 16N : 1P) (Redfield, 1958).

Unit conversions

Conversions between the light input in the FBA model, given in mmol photons gDW^{-1} hr^{-1}, and experimental measurements in μE m^{-2} s^{-1} were made following the estimations made by Shastri and Morgan (2005). They estimated that the surface area per kg of biomass was 19245m^2. However, this does not account for the change from wet biomass to dry weight for which an additional factor was introduced. Dry weight was estimated to be 51.5% of wet weight (BNID 108225, Bratbak and Dundas, 1984). Furthermore, a photosynthetic efficiency of 6% was assumed because in the model light is directed to the reaction centres immediately while experimentally we measure external light. The 94% loss accounts for the percentage of light spectrum that is photosynthetically active, reflected light, photochemical inefficiency, photorespiration and respiration; this estimation was made by Zhu *et al.*, (2008) and assumes that cyanobacteria photosynthesis efficiency is similar to that of a C4 plant. Taking all of this into account, the conversion used is that 1μE m^{-2} s^{-1} is equal to 8.07mmol photons gDW^{-1} hr^{-1}.

When investigating different nitrogen sources a maximum uptake rate per nitrogen molecule was introduced to the model. A maximum uptake rate of 0.46g N $gDCW^{-1}$ day^{-1} was used that had been measured by Kim *et al.*, (2010).

The completed model is available as an electronic resource accompanying this thesis.

Growth Assays

For the standard conditions *Synechocystis* was grown in glass microcosm vessels at 30°c and were shaken at 170 rpm. A light protocol of 14 hours light, at 5.69±1.95 μE m^{-2} s^{-1} , alternated with 10 hours dark was used. For the first growth experiment, a starting volume of 2ml per culture was used, there were 3 replicates per N source condition and the experiment lasted for 5 days. For the second experiment there was a starting volume of 5ml and there were 5 replicates per N source condition and the experiment lasted 11 days. In addition, a one week acclimation period was introduced prior to the addition of fresh media at the start of the experiment and a negative control was included that contained no nitrogen.

Synechocystis was grown in BG11 media, the content of which is below. For growth in different nitrogen sources, several modified BG11 media were made with the alternative N source while maintaining the concentration of molecular nitrogen to that of the standard nitrate media.

BG11 media final concentration:

$NaNO_3$	17.6 mM
$MgSO_4$	0.3 mM
$CaCl_2$	0.24 mM
K_2HPO_4	0.23 mM
Na_2EDTA	0.0027 mM
Ferric ammonium citrate	0.021mM
Citric acid	0.031 mM
$NaHCO_3$	0.18 mM
And trace metals	

Optical density was used as a measure of growth rate, which can be directly compared to the model predictions of biomass production. Different procedures were used as it was optimised over time. The initial readings are with an absorbance at 600nm, but later fluorescence was used with excitation at 620nm and emission at 659nm. Measurements were taken at 24hr intervals to control for circadian variation. Each density reading required sampling 200µl from each culture and this was not returned to the culture. The curves and growth rates were calculated using R.

Samples were taken throughout the growth experiment in an attempt to follow the change in arginine concentration. A Meganzyme arginine assay kit was used, however, it did not have the required sensitivity and the results were not deemed accurate enough for use.

Mass Spectrometry

Mass spectrometry was used to identify the metabolite profile of the organisms. It was performed and analysed with collaborators in the Department of Animal and Plant Sciences in Sheffield University. Direct electrospray mass spectrometry was used to

analyse the aqueous phase of the samples with a phenyalanine standard and the measurements were performed in positive mode.

The principal component analysis (PCA) was performed on the 3 biological replicates of the four nitrogen sources to test whether the sample variance was primarily correlated with the nitrogen source. One of the nitrate samples had a very low signal that was indistinguishable from background noise and was excluded from the analysis. Pair-wise comparison between all the combinations of the nitrogen sources was then performed with orthogonal projection to latent structures (OPLS) analysis. This revealed which masses significantly differed between the treatments.

Results i.) – Free-living *Synechocystis*

The project first investigated *Synechocystis* in a free-living condition in order to ensure that the model was validated by experimental results. A variety of methods were used to thoroughly check different aspects of the model: the nutrient limitation predictions were evaluated, the growth predictions on different nitrogen sources was compared to experimental data, and aspects of the model were tested with mass spectrometry data. These tests also revealed how *Synechocystis* responds to different environmental conditions.

Nutrient limitation

The FBA model was used to predict the growth rate of *Synechocystis* across different gradients of key environmental variables – light intensity, carbon concentration, nitrogen concentration and phosphate concentration. All of which can limit photosynthesis as well as other essential cellular functions, such as protein production, and thereby growth.

Growth rate was predicted across the light gradient, while nitrogen, carbon and phosphate were unbounded. The resulting light response curve is shown by figure 1. The predicted response shows the classical saturation behaviour as light stops being the limiting factor. The levels reached are unrealistically high, as nutrients have been entirely unlimited resulting in the constraint arising from the biochemistry rather than nutrients. The plateau is defined by the maximal flux through the two reaction centres, which is an arbitrary value not meant to be reached in the Knoop model. Interestingly, there is a small intermediate section which is still increasing in response to light but the benefit has decreased. In this part, the Rieske subunit of Cytochrome b6f complex has reached its flux maximum which has begun to stall the process.

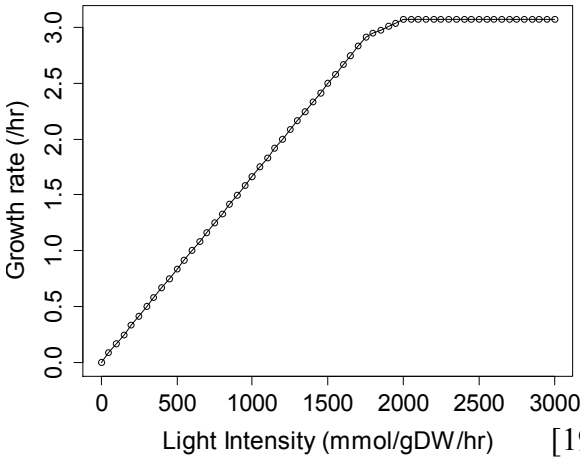

Figure 1: Predicted growth rate of *Synechocystis* across the light gradient

In a more plausible test the nutrients were constrained to realistic concentrations. To investigate the limiting factor, nitrogen and carbon concentration were plotted against each other across the light gradient (Fig. 2), while phosphate was unbounded. The model predicts that above 130mmol photons gDW^{-1} hr^{-1} (~16.1µE m^{-2} s^{-1}) further increases in light intensity no longer have any beneficial effect on growth. After this point nitrogen becomes the limiting factor, illustrated by the fact that the maximum growth rate is only achievable at the highest nitrogen concentration while it occurs across several carbon concentrations.

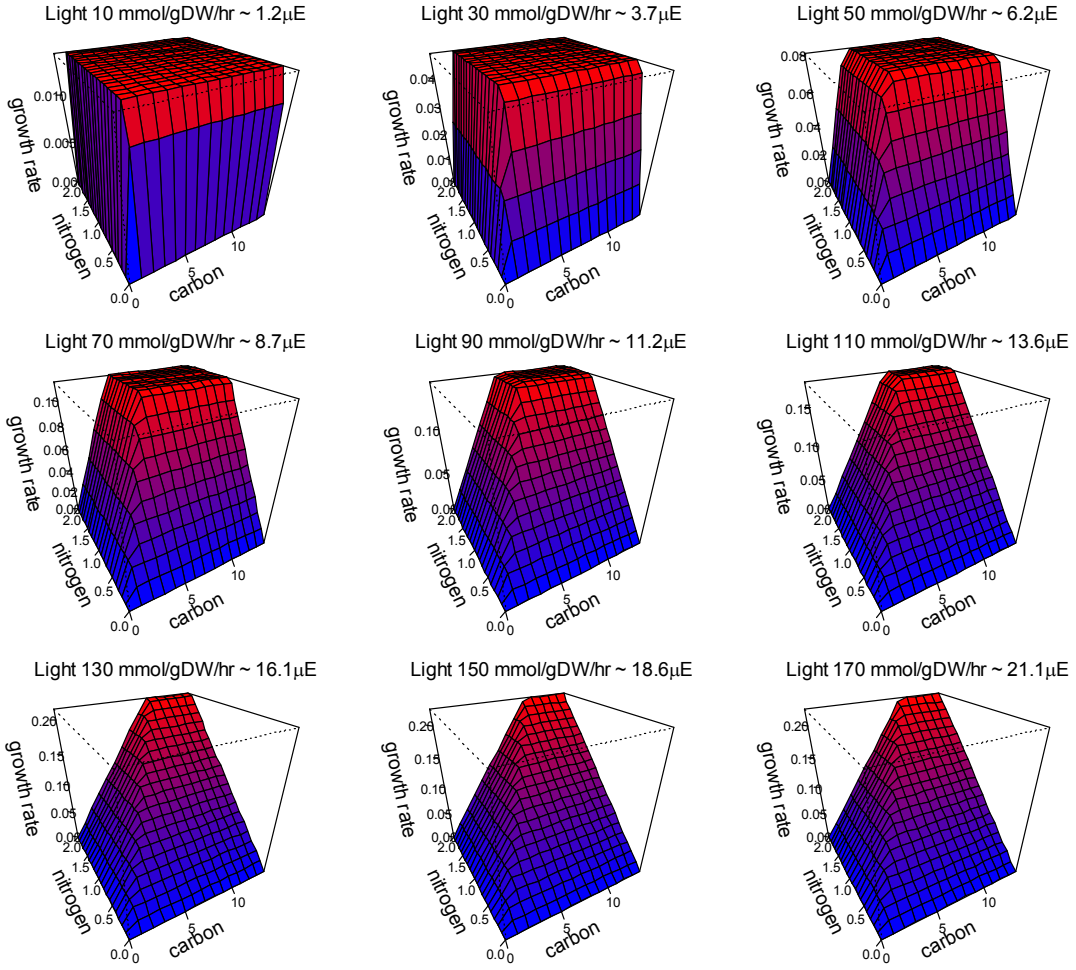

Figure 2: Predicted growth rate across the light, nitrogen and carbon gradients. Each individual plot corresponds to a set light level and varies the carbon and nitrogen available.

Then nitrogen and phosphate concentrations were plotted against each other across the light gradient (Fig. 3) while carbon was unbound. Light limitation lasts until 110mmol photons gDW^{-1} hr^{-1}, which is earlier than in the previous carbon-nitrogen case. At this stage, phosphate limitation occurs.

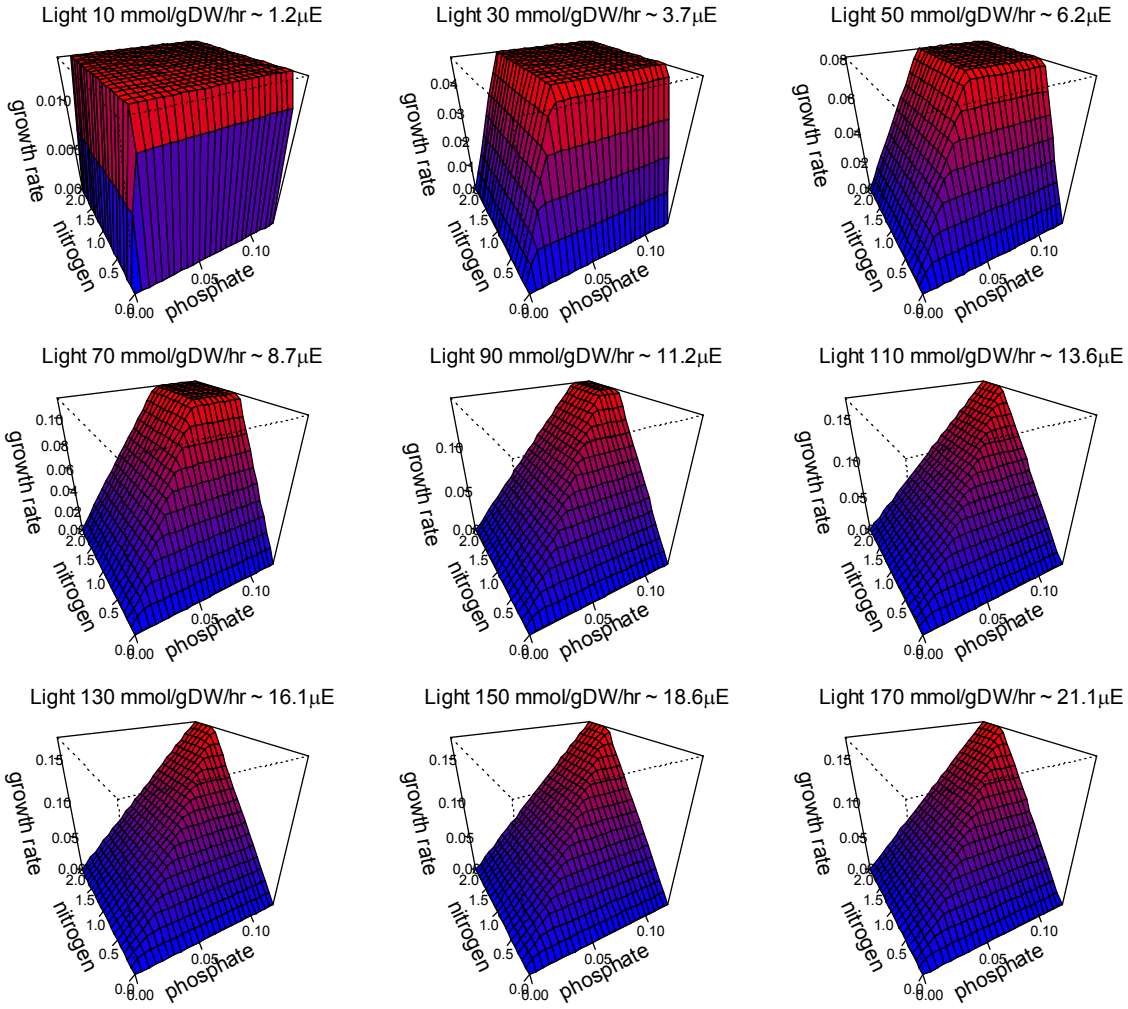

Figure 3: Predicted growth rate across the light, nitrogen and phosphate gradients. Each individual plot corresponds to a set light level and varies the phosphate and nitrogen available.

Finally carbon and phosphate concentrations were plotted against each other across the light gradient (Fig. 4) while nitrogen was unbound. Light limitation lasts until 170 mmol photons gDW^{-1} hr^{-1} (21.1μE) which is much later than in the other two limitation tests. At this stage, severe phosphate limitation occurs.

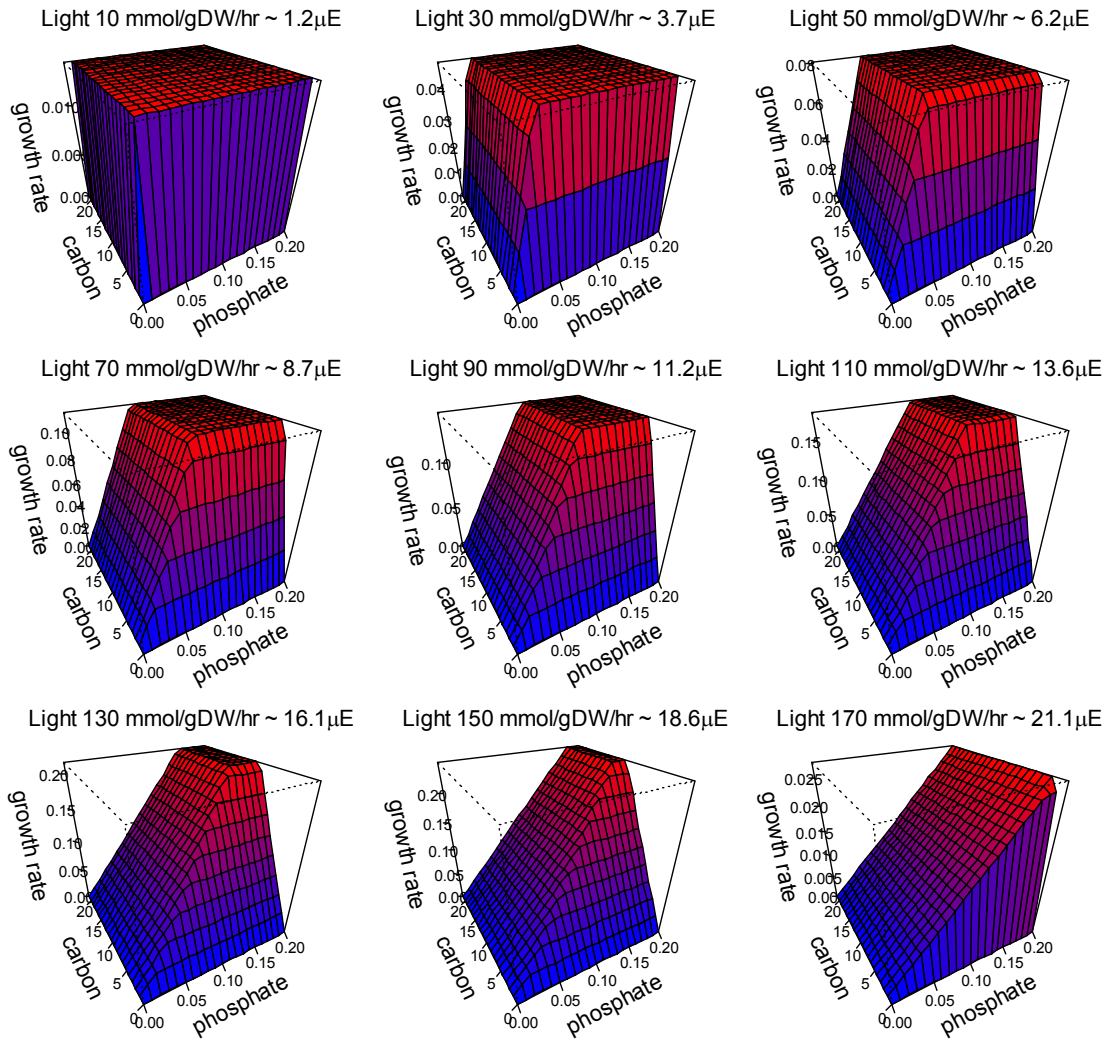

Figure 4 : Predicted growth rate across the light, phosphate and carbon gradients. Each individual plot corresponds to a set light level and varies the carbon and phosphate available.

The model, therefore, predicts that *Synechocystis* is first light limited, then phosphate limited and then nitrogen limited. However, these results are very reliant on the concentration ratio used, which was the Redfield ratio (106 C : 16 N : 1P). The Redfield ratio is the average for environmental aquatic conditions, and matches the ratio within the phytoplankton community. It is often a good average, however, it is not specific for *Synechocystis.* Particularly as *Synechocystis* is a freshwater cyanobacterium and the Redfield ratio has been demonstrated to be less applicable to freshwater environments because they have more variable nutrient levels (Hecky *et al.*, 1993). If the concentration ratios are altered, different limitation patterns occur, for instance, if the

C:N ratio is decreased from 6.625 (Redfield value) to 4.55 then carbon and nitrogen are in balance and neither limits more than the other. Similarly for nitrogen and phosphate if the ratio is decreased then a balance is reached, and if it is further decreased nitrogen becomes more limiting than phosphate.

The nutrient ratio can be used to define the conditions when each nutrient would be limiting by finding the ratio at which the exact balance occurs. These were found and are shown in Table 1. As the balance ratios found do not match those of the Redfield ratio, the model predicts that *Synechocystis* deviates significantly from this average stoichiometry.

Ratio	Ratio < Balance	Balance point	Ratio > Balance	Light limitation till (mmol photons gDW^{-1} hr^{-1})
C:N	<4.55 Carbon limits	4.5	>4.55 Nitrogen limits	130
N:P	<12.5 Nitrogen limits	12.5	>12.5 Phosphate limits	110
C:P	<56.5 Carbon limits	56.5	>56.5 Phosphate limits	170

Table 1. Summary of nutrient concentration ratios and their impact on nutrient limitation.

If the environmental ratio is known these determined ranges can be used to predict the limiting nutrient. For instance, *Synechocystis* is grown in BG11 media that has a N:P molar ratio of 76.829 (3 d.p) indicating the phosphate is more limiting than nitrogen. The carbon source is from CO_2 that dissolves and reacts to form carbonic acid, (H_2CO_2), bicarbonate (HCO_3^-) and the carbonate ion (CO_3^{2-}). From a Bjerrum plot for carbonate it is evident that at pH 7 80-90% of the dissolved carbon is in the bicarbonate state. It is estimated that at normal atmospheric partial pressures and at 25°c, a freshwater solution with pH 7 will contain 4.79×10^{-2} mM HCO_3^- (equilibrium constants taken from Lower n.d). Under these assumptions, BG11 media has a C:N of 0.00271 and a C:P of 0.208, revealing that is severely carbon limited. This matches multiple reports from the literature (Kim *et al.*, 2010 and Wang *et al.*, 2004), including the common practise of increased CO_2 as a growth condition (Martinez *et al*, 2010 and Allahverdiyeva *et al.*, 2011).

In this way, understanding the nutrient limitation behaviour can predict how *Synechocystis* will respond in different conditions, and could even be used to improve laboratory growth rate by addressing the identified limitation.

Synechocystis **Composition**

The relevance of an FBA model to reality is highly dependent on the accuracy of the biomass function, particularly when it is set as the objective function and therefore is critical to the predictions. The major components in the biomass function in the Knoop model are shown in Table 2, these are based on the biomass function used by the original Shastri and Morgan (2005) model. Additional detail, not shown below, is provided for the identities of the compounds within the major components (i.e. the fractional composition of the amino acids within the protein group). These were based on bioinformatics estimations by Nogales *et al.,* (2012) who followed the standard protocol of Thiele and Palsson (2010).

Component	% composition from Shastri and Morgan	Requirement (mmol gDW^{-1} hr^{-1})
ATP		53.35
H20		53.35
Proteins	51	0.51
DNA	3	0.031
RNA	17	0.17
Carbohydrates	19	
Cell Wall		0.059
Lipid	10	0.12
Metabolite pool		0.029
Ions		0.01
Pigments		0.0244
Glycogen		0.21031

Table 2: The main components of the biomass function from the original Shastri and Morgan model and the Knoop model.

To verify the basic assumptions of the biomass function mass spectrometry was performed.. A non-targeted approach was used with direct-injection electrospray (ESI) mass spectrometry to get a rough spectrum (Fig. 5). The estimated identities of the major peaks were compared to the composition in the model.

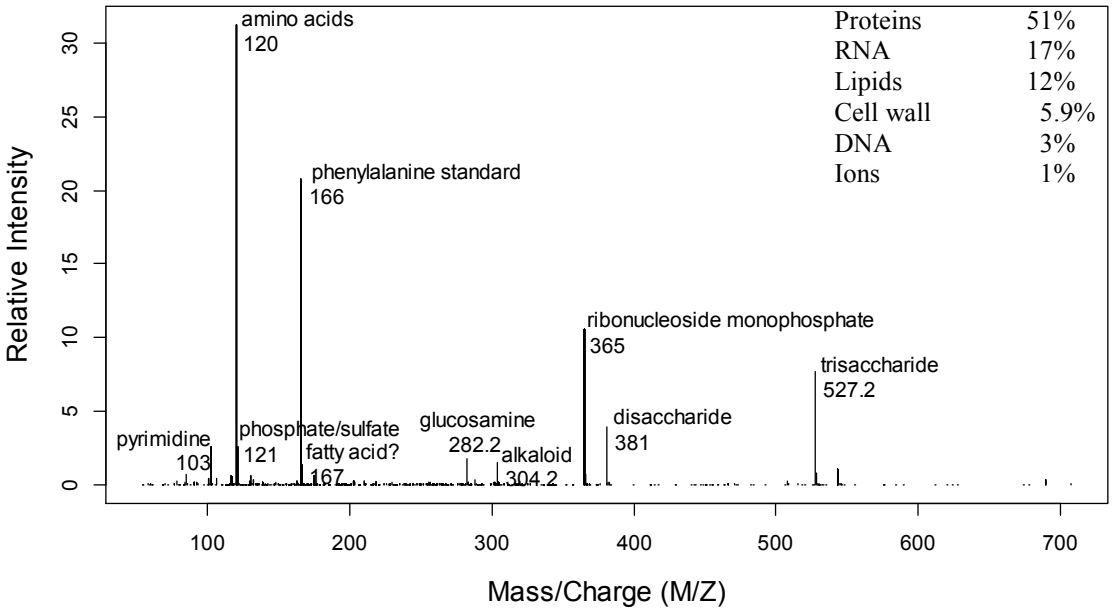

Figure 5: Mass spectrum of *Synechocystis*. The values in the top left corner represent the major parts of biomass composition assumed by the model expressed as a percentage.

The amino acid peak is the largest which matches the model though its relative intensity is less than the model's 51% value. The next largest peak is estimated to be the ribonucleoside monophosphates and would therefore represent the RNA peak. The cell wall fraction might be represented by either the trisaccharide or disaccharide carbohydrate peaks, as the long cell wall polymers fragment. The pyrimidine peak is a close match to the DNA fraction. The peak for the inorganic ions (labelled as phosphate/sulphate) is a bit higher than predicted but this could be contaminated by the ions used in the ionisation step. The lipids are not represented, except for a very small fatty acid peak. This is expected because this analysis was performed on an aqueous phased extraction sample, and the lipids are more likely to be in the chloroform phase.

These results support the basic composition of the model's biomass. There are differences in composition but considering that this is a non-targeted spectrum these are within an acceptable range. Importantly, the relative composition is the same. To fully verify the biomass composition exact identities of the relevant peaks would be necessary, which would involve MS-MS work.

Different Nitrogen Sources

The FBA model was used to predict the growth rates on a range of nitrogen sources. A series of different sources was tested to represent the major forms of organic nitrogen used by phytoplankton. It also included the hypothesised nitrogen sources in the *Paramecium-Chlorella* symbiosis. Guanine was included despite the fact that the enzymes necessary for its uptake and conversion (a purine transporter and guanine deaminase) have not been identified in *Synechocystis* (Solomon *et al.*, 2010). However, since it is a candidate source for *Paramecium-Chlorella* it was of particular interest and other cyanobacteria do have the required enzymes, therefore it is possible that they have simply not been identified yet.

The predicted growth rates are shown in Figure 6a. Glutamate is predicted to be the most effective source in terms of growth rate. Growth on nitrate is predicted as being the slowest. These values make sense biologically as they match the requirement of cellular processing before the nitrogen is available. For instance, nitrate is reduced to nitrite and then to ammonium but if ammonium is supplied directly the first two stages are bypassed which conserves the cell's reducing agents. The amino acids are the most energy efficient as the GS-GOGAT pathway is unnecessary, which incorporates ammonia into amino acids and requires ATP.

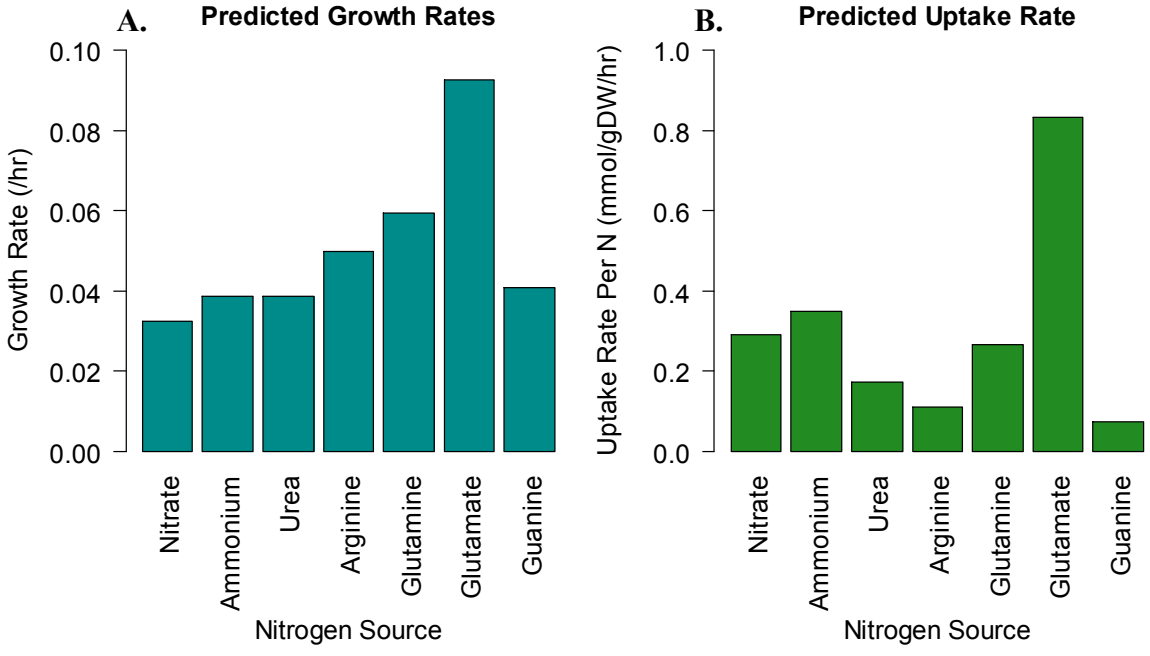

Figure 6: FBA predictions for *Synechocystis* grown on different nitrogen sources. A) Plots the predicted growth rate and B) plots the predicted uptake rate per N molecule of the nitrogen source.

In addition, the uptake rate of the nitrogen source was predicted (Fig. 6b). The results clearly indicate the glutamate has a much higher uptake rate than the other sources, while arginine and guanine have very low uptake rates. Arginine supports a high growth rate despite its low uptake rate, indicating that it is an efficient source. This is perhaps expected given the fact that it has 4 nitrogen atoms and therefore is the most nitrogen-rich source. The higher uptake of glutamate may be facilitated by its low processing cost, which may be restraining the other sources. None of the sources reach the maximum uptake rate imposed, which is taken from experimental work in the literature (see the Methods section).

In order to test these predictions, *Synechocystis* was grown in media providing these nitrogen compounds as the sole N source. The growth curve across the 120hr experiment is shown in Figure 7.

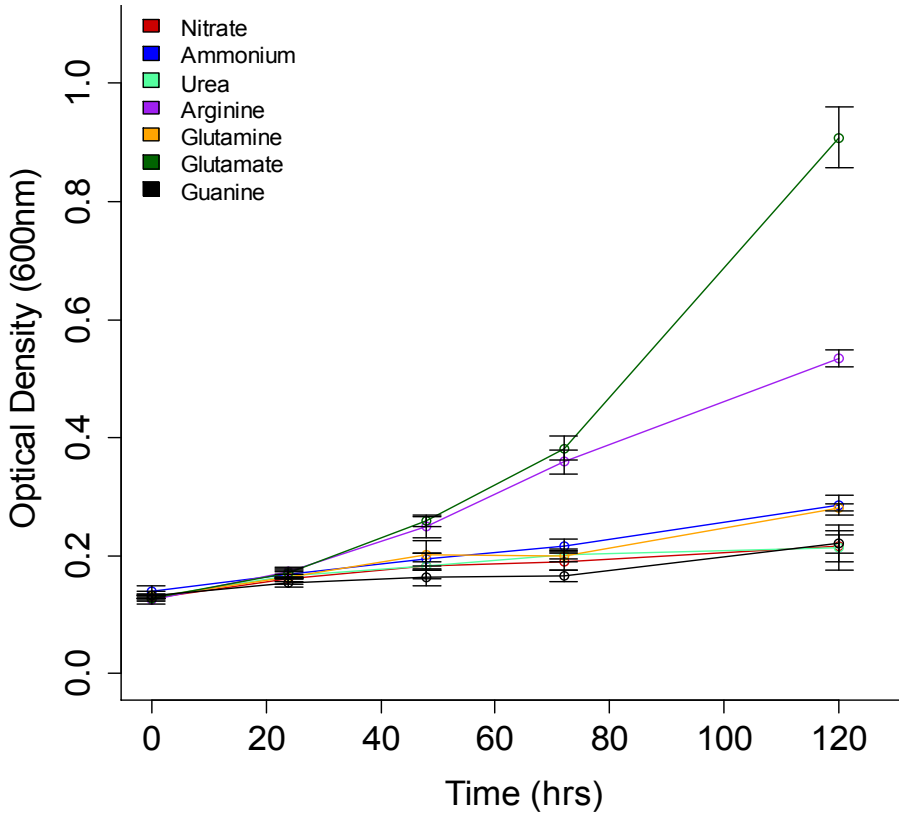

Figure 7: *Synechocystis* growth on different nitrogen sources measured by optical density with standard error bars plotted.

From the experimental data the initial growth rate was calculated based on the results for the first 48 hours. Longer term growth rates were not calculated as the different sources appear to fit different models (glutamate appears exponential, ammonium is perhaps linear). This means that different calculation methods would be needed for the

different sources, which would have led to inconsistencies. The experimental growth rates were compared to those predicted by the model (Fig. 8). A scaling factor was applied to the model predictions based on the nitrate baseline, without which the predictions are higher. This scaling factor effectively accounts for the transporter uptake rate because such enzyme dynamics are not included in FBA modelling. In the comparison the relative behaviour across the sources is fairly well matched. Applying a Student's T test finds that for only two sources are the model predictions significantly different to the experimental values – for ammonium (one-sample t-test, $t(2) = -4.9$, $p = 0.039$) and glutamate (one-sample t-test, $t(2)= -15.9$, $p = 0.004$). Even for these, the predictions are still qualitatively accurate, since the model correctly predicted glutamate would lead to the highest growth rate. Furthermore, the values at the end of the experiment (Fig. 7) show that the difference between arginine and glutamate increases, which is more align with the predictions. Arginine is the only case where the experimental value is higher than the predictions.

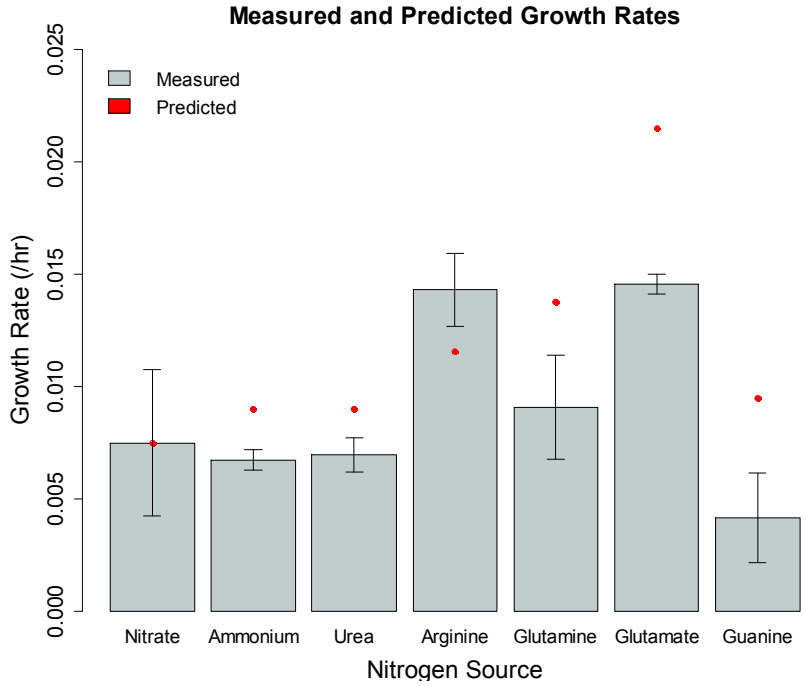

Figure 8: FBA predictions compared to experimental results for *Synechocystis* growth rate on different nitrogen sources with standard error bars plotted.

The experiment was repeated in an effort to improve precision and check the results. In order to increase replication the second test focused on a few key sources - nitrate, arginine and glutamate. The growth data is shown below (Fig. 9). Only nitrate had a significant difference between the predictions and the experimental growth rate (one-sample t-test, $t(4) = -5.1$, $p = 0.007$). This is because the growth on nitrate is unexpectedly poor and plateaus very quickly. Given that nitrate is the standard nitrogen

source for *Synechocystis* growth, this seems implausible and is perhaps due to experimental error.

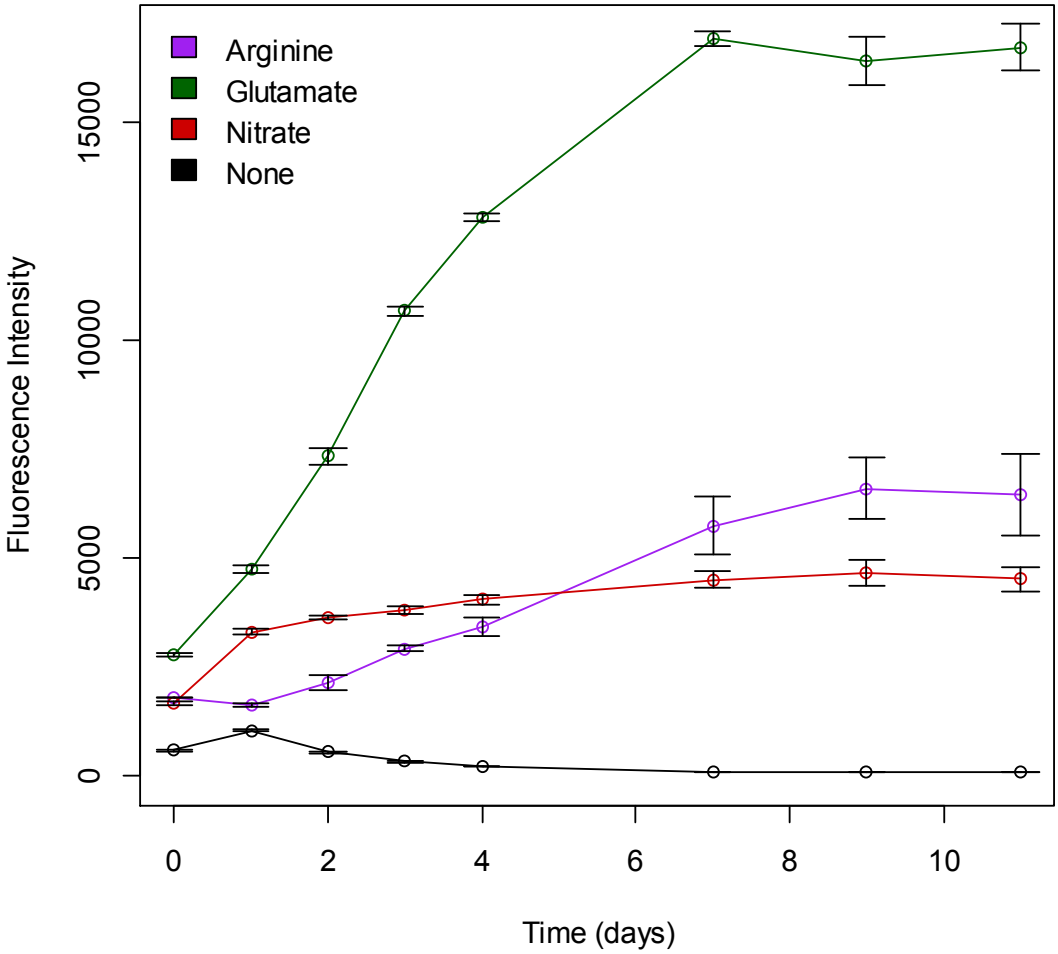

Figure 9: Second experiment with *Synechocystis* growth on different nitrogen sources measured by fluorescence and with standard error bars plotted.

Unlike nitrate, the glutamate and arginine results are that of expected growth curves. Glutamate performed consistently as the most efficient nitrogen source. Arginine has a lag period after which it supports growth. This slow inducement could indicate a period of metabolic adjustment, this fits with the model prediction discussed in the next section. Growth rates were calculated but because of the lag for arginine this was done over different time periods (glutamate was calculated between day 1 to 3 and arginine between day 1 to 7). The ratio between the glutamate and arginine growth rates is 1.97 and is very close to the ratio between the FBA predicted rates, which is 1.86.

These results have predicted and tested how *Synechocystis* responds to different nutrient sources. The model seems capable of qualitative predictions though it has some disparities.

The Effect of Different Nitrogen Sources on Metabolism

Changes in the nitrogen source would be expected to cause changes in metabolism, as different assimilation pathways are necessary. The FBA simulations for the different nitrogen sources can be investigated further by exploring the variance in pathway fluxes rather than just using the growth rate output (Fig. 10). The model predicts that *Synechocystis* metabolism is similar across some of the nitrogen sources, but between others there are large differences. Ammonium and urea behave identically, because urea can be converted to ammonia with urease and this only requires a water molecule (Solomon *et al.*, 2010). They are also similar to nitrate because the major pathways used are the same, though the flux rate differs. The amino acids on the other hand have varied pathway use, revealing that the nitrogen source has large implications for *Synechocystis's* metabolism.

The variance of pathway fluxes for the most divergent sources is shown by Figure 10. It focuses on the glycolysis pathway and the TCA cycle. The TCA cycle is expected to be incomplete when photosynthesising and therefore the TCA cycle is used for the production of intermediates rather than energy. However, when grown on glutamate the cycle is effectively complete though the unusual inclusion of a proline hydroxylase. This enzyme, however, was included in the model on BLAST similarity data only and has not been confirmed as present.

Furthermore, the TCA cycle and glycolysis have been decoupled in the glutamate condition, demonstrating that the carbon in glutamate is sufficient to drive the TCA cycle when light. This results in the output from photosynthesis being entirely driven towards carbon storage.

Across the other nitrogen sources there are differences between which parts of the cycle are unused. For instance, arginine, unlike all of the other sources, has no flux between oxaloacetate and 2-oxoglutarate but it does have flux between 2-oxoglutarate and succinate, which is not seen for any of the other nitrogen sources. This is using a unique cyanobacteria TCA bypass that the Knoop model introduced, which involves two newly identified enzymes (OGDC and SSADH) for the conversion (Zhang *et al.*, 2011).

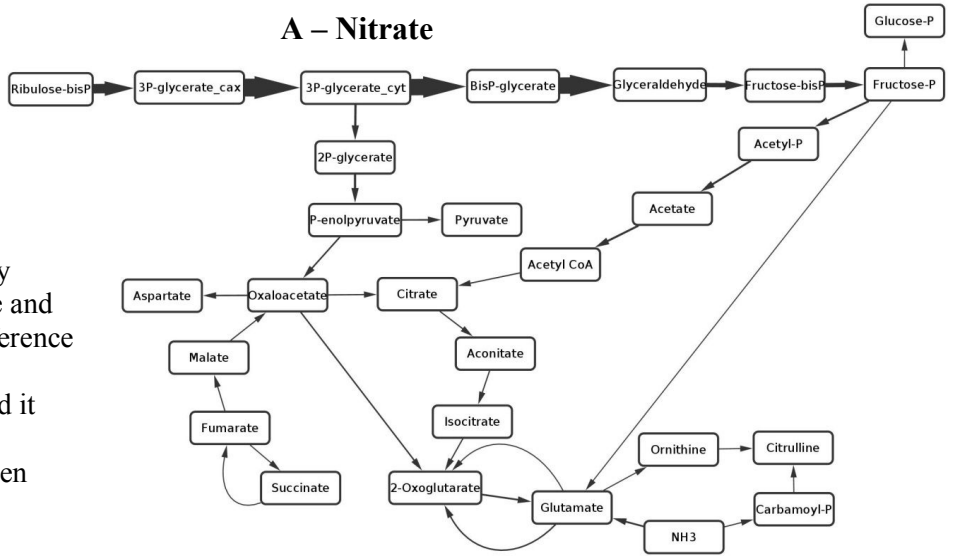

Figure 10: FBA predictions of pathway fluxes when grown on nitrate, arginine and glutamate. The fluxes are drawn in reference in the standard condition of nitrate. If relative to nitrate, a compound is added it has been highlighted in red and if a compound has been excluded it has been greyed out.

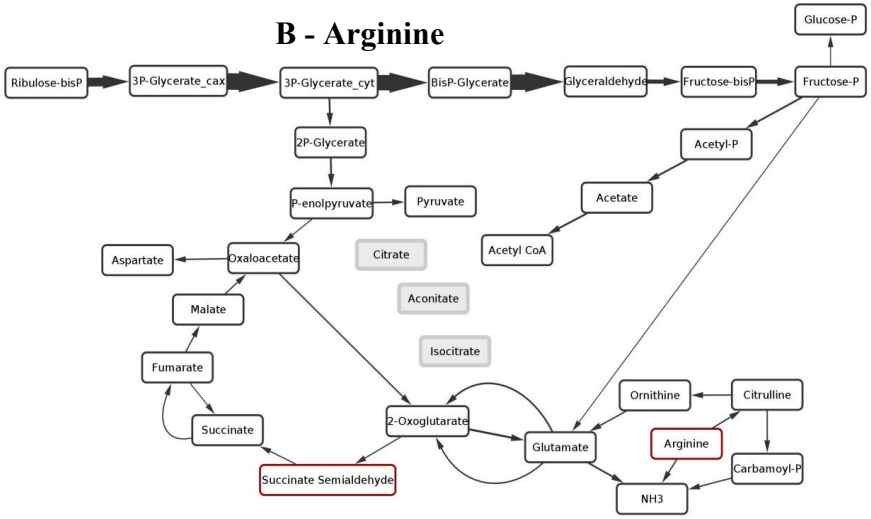

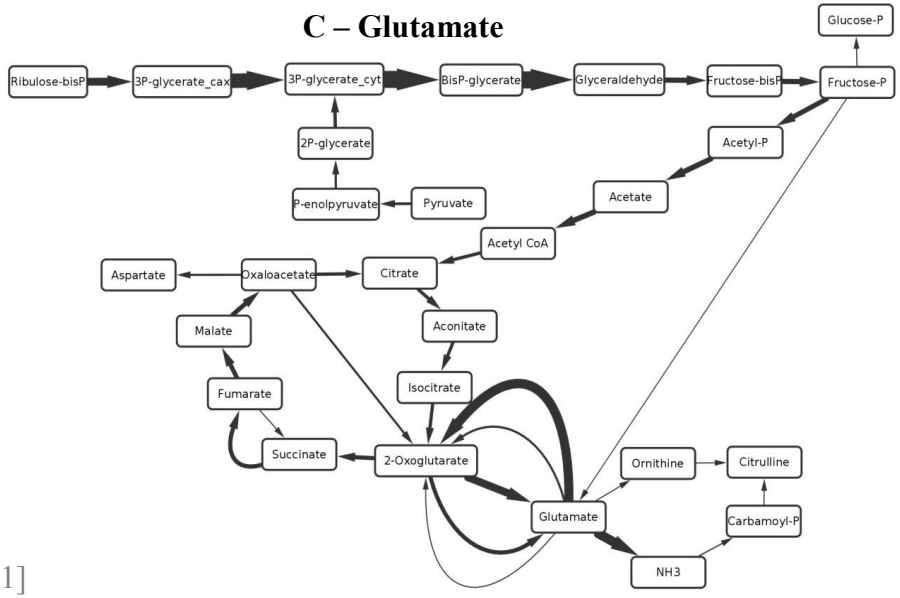

The flow in glycolysis comes from the output of photosynthesis as glycerate-3-phosphate and then in most cases splits, with the majority of the flux going through glycolysis in reverse to form glucose and feed into carbon storage as glycogen. The remaining flux is directed to phosphate-enolpyruvate/pyruvate.

These predicted changes to metabolism can be tested with mass spectrometry. Samples from cultures grown on the different sources were analysed with ESI mass spectrometry on the aqueous phase. The ion counts were compared between the different samples and the result is shown in Figure 11 as a PCA plot. The data groups with reasonable accuracy according to the nitrogen source with the exception of an arginine sample that may be an outlier or in an earlier stage of metabolic adjustment, which could correspond to the lag phase seen in the experimental results.

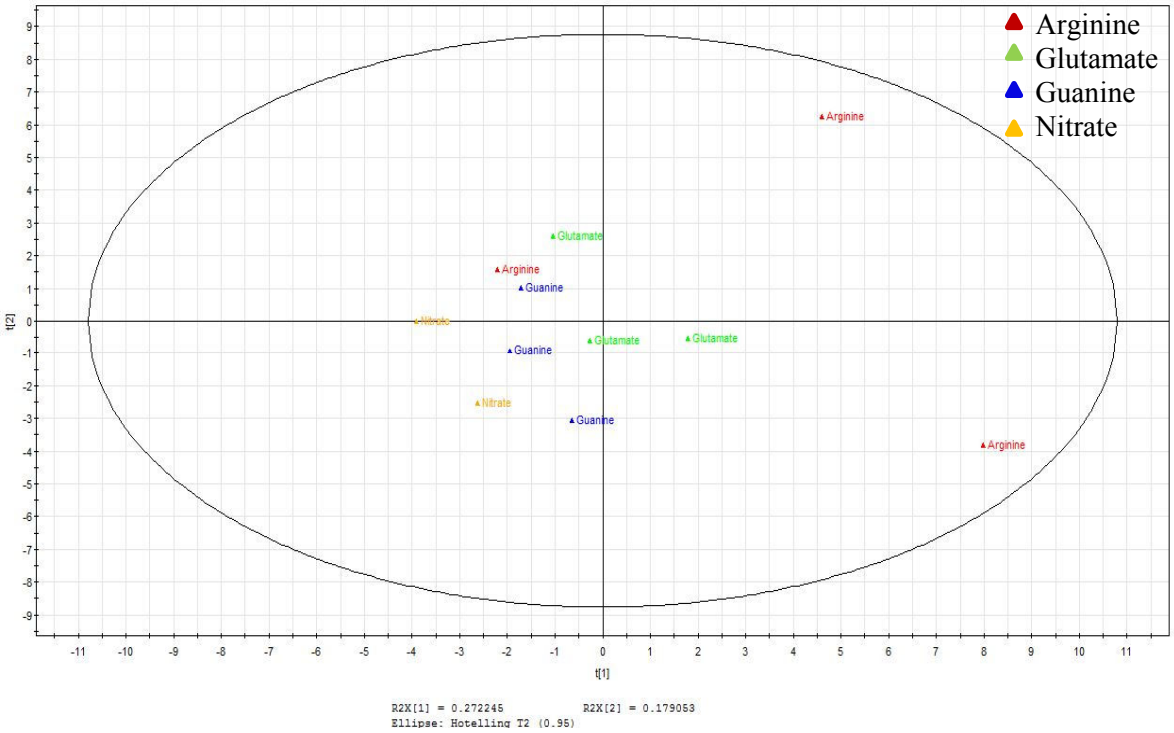

Figure 11: PCA plot comparing the mass spectra from samples grown on the different nitrogen sources.

This indicates that the between group variation is greater than the within group variation, and implies that there are distinct metabolic profiles for the different conditions.

The key metabolites that define the different groups can be identified by doing pairwise analysis, which can be visualised with OPLS plots. The pair with the biggest difference in metabolism was arginine and nitrate, and their OPLS plot is shown below (Fig. 12).

The first plot shows the negative side of the plot (Fig. 12a); these metabolites are therefore significantly decreased in the arginine condition compared to nitrate. Whereas, in the second (Fig. 12b) the positive side is shown, which shows those metabolites that are increased in arginine compared to nitrate. When the error bar does not cross the 0 line the difference in intensity is significant.

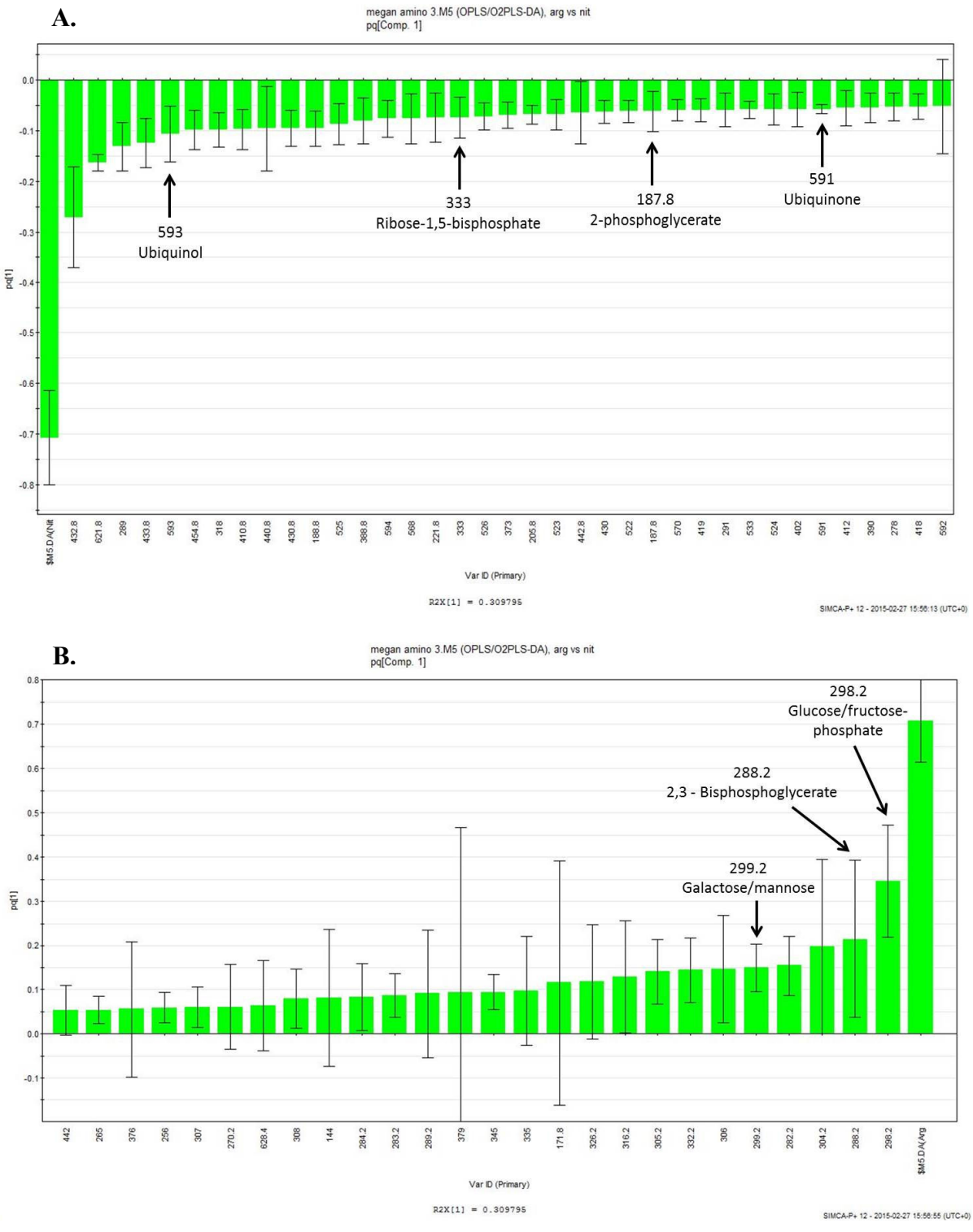

Figure 12: OPLS plots of arginine against nitrate. A) the negative part of the plot B) positive side of the plot. Estimated identities for metabolites of interest are labelled.

The significant masses were compared to a compiled mass list to estimate the metabolite identity, in some cases there were many candidates therefore no clear conclusion could be drawn. The most interesting estimates have been labelled on the plots. In particular, 2,3-bisphosphateglycerate and fructose-phosphate/glucose–phosphate were increased in arginine. This is indicative of glycolysis having a greater flux, which fits the model predictions of a higher flux through reverse glycolysis. Nitrate, however, has increased 2-phosphoglycerate which is also in glycolysis but it is in the lower section following the output from photosynthesis. Therefore it may be that different sections of glycolysis respond differently. In addition, ribose-1,5-bisphosphate was increased in nitrate, this may indicate a higher rate of photosynthesis. Though not predicted by the model, this is logical because the amino acid sources provide organic carbon as well as nitrogen, which may allow photosynthesis to decrease while still maintaining growth. Furthermore, there is an increase in ubiquinol in the nitrate condition, which is the primary electron carrier in respiration and therefore this indicates an increase in oxidative phosphorylation.

Unfortunately at this stage, no TCA cycle compounds were identifiable in the OPLS plots. Looking specifically for these masses in the entire spectrum it is possible to find candidates, for instance a likely malate signal has been found. Unfortunately, there are two signals very close to the succinate semialdehyde potential mass, which means that further analysis by MS-MS is required to identify which, if any of these, corresponds to succinate semialdehyde. Once identified, this would reveal whether that cyanobacteria TCA bypass was used when grown on arginine.

For an accurate comparison of the metabolism between the conditions the key compounds need to be identified robustly. Without such support these comparison remain speculative and it is not possible to say whether or not the model predictions for the difference in pathways used is correct. For now, it is clear that the nitrogen sources lead to clear distinctions in their metabolite profile, and this does seem to involve the main cellular pathways, particularly glycolysis.

Through these approaches it has been demonstrated that the model can accurately predict *Synechocystis* nutrient limitation, its growth rates in novel conditions and it appears its predictions are valid to a pathway-level resolution. Furthermore, the biomass upon which the model rests has been validated. Overall this provides strong

endorsement for the free-living model, and this provides support for its extension to novel scenarios.

Results ii.) – Becoming Symbiotic

The previous work has examined *Synechocystis* in a free-living situation and in doing so has verified the model by a number of different approaches. The next step was to extend the model to the context of endosymbiosis, and therefore to predict how such transitions can occur.

Initially, as an intermediate step, a partially symbiotic state was created. This was done for the different nitrogen source comparison because in the endosymbiosis the main exchange into the symbiont is nitrogen. Some of the nitrogen sources contain carbon and therefore the host, who is providing the nitrogen, is giving carbon away in order to receive carbon. The earlier situation modelled a free-living and therefore 'selfish' *Synechocystis*, which prefers the source that enhances its growth the most. However, carbon compensation can be introduced to model a mutualistic situation, in which the *Synechocystis* does not benefit from this carbon. This models a situation when the carbon within the nitrogen source is effectively returned to the host; therefore the model is transitioning from a 'selfish' state to a cooperative one.

When carbon compensation is applied (Fig. 13) the predicted growth rate across the nitrogen sources is now similar and the advantage of glutamate is hugely diminished. This is because the *Synechocystis* is no longer gaining the benefit of any carbon within the nitrogen source and glutamate has the highest C:N ratio. Arginine and ammonium now act as the best nitrogen sources.

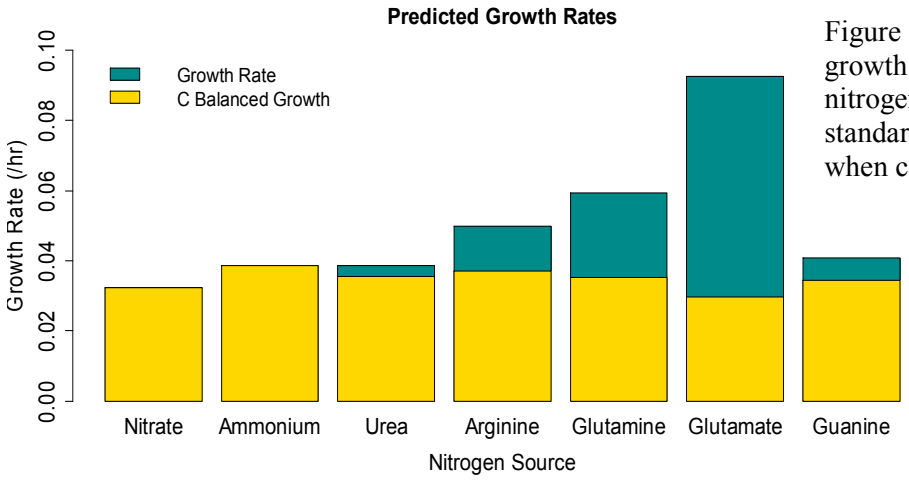

Figure 13: FBA predicted growth rates on different nitrogen sources in the standard condition and when carbon compensated.

Carbon Export

A full symbiotic state was then enforced by including a complete exchange reaction; therefore, in order for *Synechocystis* to uptake nitrogen it must export carbon. An example of which is shown below (reaction 3). The ratio of carbon to nitrogen exchange, effectively the relative worth of these elements, was estimated using a C:N ratio from a ciliate, *Paramecium caudatum*. A ratio of 3.5 was used according to measurements by Finlay *et al.* (1981). This is based on the assumption that the host is primarily in control and would ingest bacteria that did not cooperate. This value, along with any carbon compensation, forms the parameter value for the carbon export compound. Furthermore, all calculations are based on the number of carbon or nitrogen molecules within the compound.

Reaction 3: $0.583*Glucose_{[cyt]} + Nitrate_{[ext]} + ATP_{[cyt]} + H_2O_{[cyt]} \longrightarrow$

$0.583*Glucose_{[ext]} + Nitrate_{[cyt]} + ADP_{[cyt]} + Orthophosphate_{[cyt]}$

The model was then used to predict the identity of the carbon export compound. Representative carbon compounds were chosen (Fig. 14) that span from the output of photosynthesis to the storage compound of *Synechocystis*, glycogen (Yoo *et al.,* 2002). Pyruvate was also included because of its pivotal role in carbohydrate metabolism.

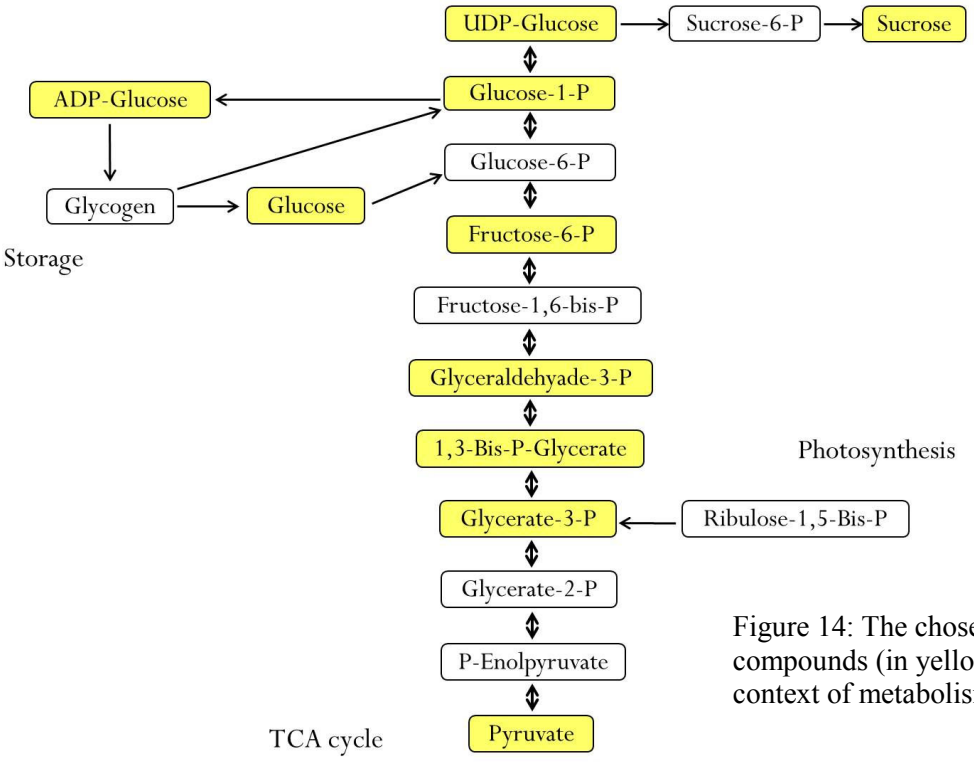

Figure 14: The chosen carbon compounds (in yellow) in the context of metabolism

The selected compounds were first exchanged for the standard nitrogen source, nitrate. The predicted growth rates are all very similar (Fig. 15a). For this analysis, any carbon compound containing phosphate was also tested in a phosphate antiporter situation. This allows for any phosphate to be regained, which otherwise increases the cost of the exchange. This is a plausible addition because an antiport mechanism is theorised to have facilitated exchange in the primary endosymbiotic event (Weber *et al.,* 2006) and phosphate antiporters are currently present in the exchange between chloroplast and the cytoplasm (Flügge *et al.*, 1991). It is evident that the phosphate antiport makes a significant difference, especially for ADP-glucose that cannot grow without it. The different uptake rates (Fig. 15b) suggest that the higher uptake is used as compensation for when there is no antiport mechanism. This is shown by UDP-glucose. Overall, pyruvate exportation leads to the highest growth rate of *Synechocystis* though there is very little variation.

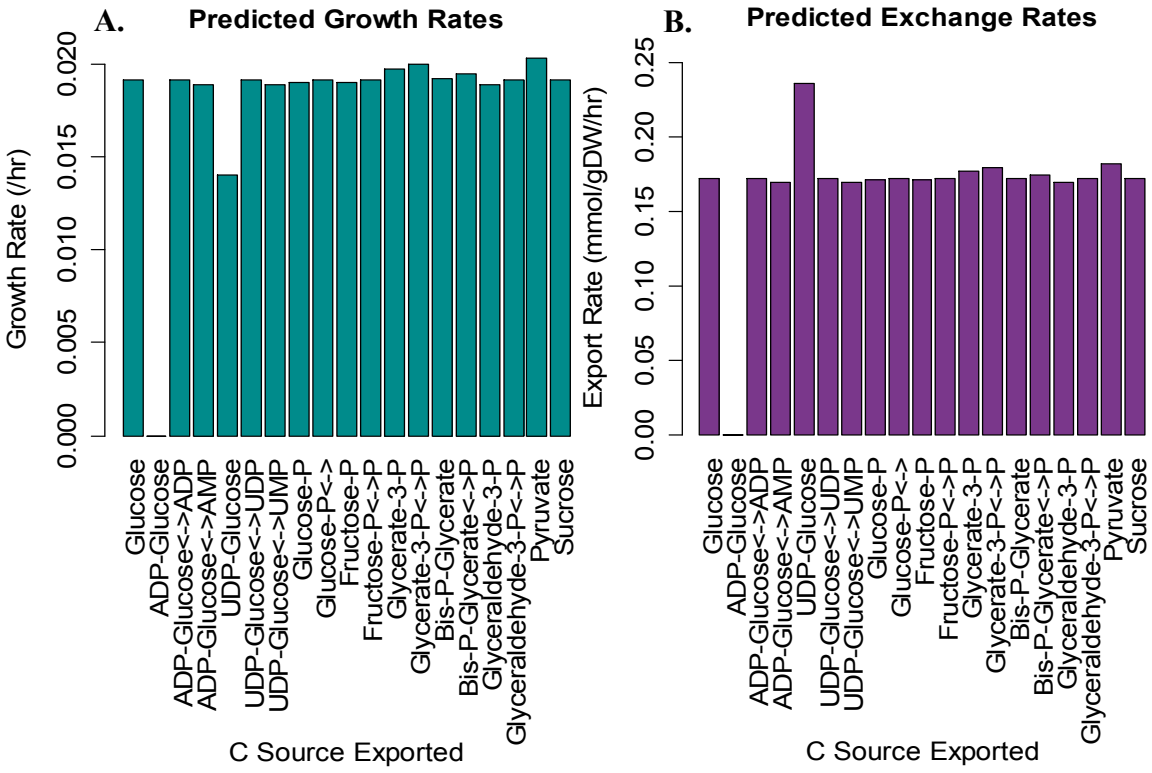

Figure 15: FBA predictions for different carbon export compounds. A) plots the predicted growth rate values and B) the predicted nitrogen uptake flux

Combinatorial Exchange

The analysis was then expanded to consider the range of carbon sources in combination with the range of nitrogen sources (Fig. 16). The nitrogen sources have been arranged on the X axis in order of increasing growth rate from left to right when exchanged for glucose, to allow easier comparisons. The results are not merely additive and the sum of the two previous tests, but rather some of the combinations behave non-additively. Pyruvate is unusual because it is the only carbon for which arginine and not ammonium results in the highest growth and for which glutamate does not lead to the lowest growth rate. UDP-glucose has much larger differences between the nitrogen sources and there is no growth if it is exchanged for glutamate. In this analysis, the nitrogen sources are carbon-compensated because at this stage we are modelling a fully cooperative exchange. This is why glutamate leads to low growth rate. This combinatorial analysis predicts that a pyruvate for arginine is the optimal exchange when the relationship is mutualistic.

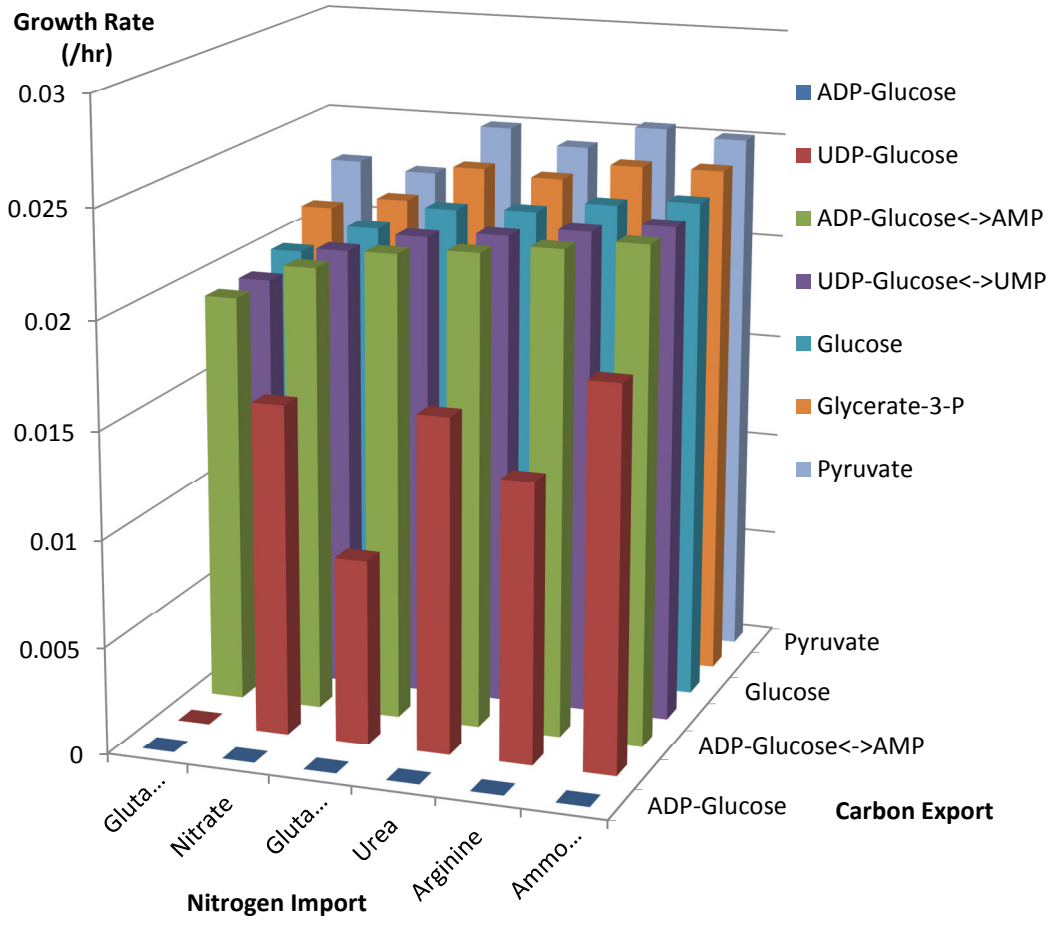

Figure 16: Predicted growth rates of the different combinations of the nitrogen import compounds and the carbon export compounds.

This analysis was performed with a set C:N ratio that assumed the host was in control and therefore sets the relative value of the nutrients. This is the likely 'endpoint' in the endosymbiosis as the host could egest/digest any uncooperative symbionts that did not adhere to the 'set price'. However, it may be that in the transitional stages the symbiont retains a degree of autonomy and therefore has more influence on the price.

To investigate the effect of the C:N ratio and therefore the price, the optimum metabolite exchange was identified over a range of ratios and also over a degree of carbon compensation (from 0 to 100%) (Fig. 17). The gradient lines indicate the value of *Synechocystis's* growth rate. The space between a pair of contour lines represents a change in growth rate of 0.0045 mmol biomass gDW^{-1} hr^{-1}. As both the C:N ratio and carbon compensation increases the symbiosis becomes more costly for the symbiont and more beneficial to the host. Interestingly, the transitions between carbon sources are dependent on the C:N ratio, but the transitions between the nitrogen sources are not and instead occur at set percentages of compensation. As the ratio and therefore price increases the transition to using pyruvate as the carbon export compound is made faster. Pyruvate contains no phosphate or nitrogen unlike UDP and ADP, therefore it may be that the cost of these additional molecules intensifies at higher ratio values.

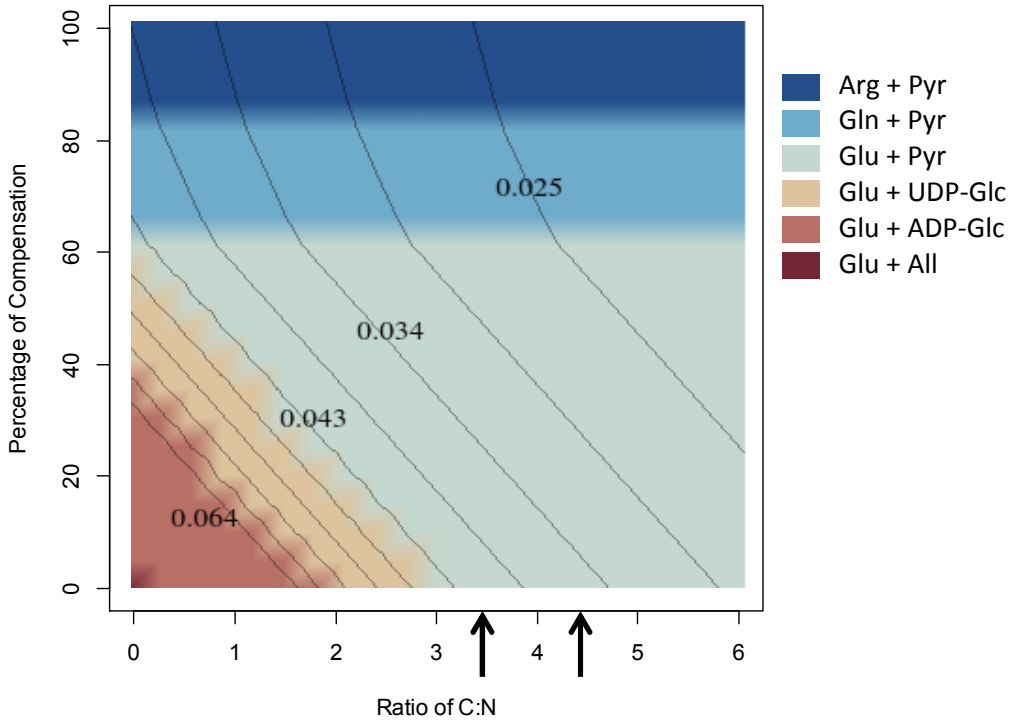

Figure 17: Optimal metabolite exchange across a range of ratios and degrees of carbon compensation. The arrows indicate the C:N ratio of the two organism; 3.5 is the value for the host and 4.5 for the symbiont. Plotted in mathematica 9.0.. The abbreviations used are: arginine (Arg), glutamine (Gln), glutamate (Glu), pyruvate (Pyr), UDP-glucose (UDP-Glc), ADP-glucose (ADP-Glc) and the entire group of carbon compounds tested is referred to as 'All'.

The C:N ratio of *Synechocystis* predicted by the nutrient limitation work is 4.5, while the host ratio used earlier is 3.5. The graph demonstrates that the change between these two values is very little, with no difference between their transition points. This implies that to adapt from a free-living directed state to one where the host imposes control over the relative value of C:N is plausible and in this aspect does not require much adjustment.

The symbiotic model has revealed that the metabolic exchange is dependent on the nature of the symbiosis. With the optimum exchange metabolites changing when the symbiont is ‘selfish’ or mutualistic.

Discussion

This project took the novel approach of applying FBA to model an evolutionary transition to endosymbiosis. Following an investigation into the free-living state of the cyanobacterial symbiont, predictions were made that charted the transition to endosymbiosis. The work focused on the metabolic changes that would occur, in particularly in terms of the exchange reaction at the heart of the symbiosis. It accounted for both the symbiont, whose metabolism was modelled directly, but also considered the interests of the host through the 'price' of the compounds and compensation costs. In doing so, FBA modelling has been used to predict the metabolic transitions that may have occurred in an ancient evolutionary event.

The predicted optimal exchange metabolites are known to be exchanged in some natural endosymbiosis. For instance, glutamate, along with glutamine and aspartate, is provided by the aphid to its bacterial endosymbiont (Sasaki *et al.*, 1995; Thomas *et al.*, 2009). Arginine metabolism, however, is often associated with symbioses without it being the actual exchange metabolite, for instance in the arbuscular mycorrhizal symbiosis arginine is converted to ammonium just before being exchanged (Fellbaum *et al.*, 2012). In addition to this example, ammonium is the nitrogen exchange metabolite in several other symbioses, including *Gunnera-Nostoc* (Silvester *et al.*, 1996), salamander eggs and green algae (Small *et al.*, 2014) and Rhizobia and legumes (Prell & Poole, 2006). Ammonium, unlike arginine, does not contain any organic carbon; it could, therefore, be that the model's carbon compensation mechanism is only partially able to account for this cost to the host. Since the model only indirectly models the host this is perhaps unsurprising. Ammonium was predicted as being the second-best metabolite after arginine, but evidence from natural endosymbioses implies that when the host's interests are fully taken into consideration, this balance changes and ammonium is preferred. This assumes, however, that the exchange will be similar to current symbioses and it may be the case that during the early stages of its coevolution a *Synechocystis-Paramecium* endosymbiosis may have used an exchange reaction that is uncommon in more evolutionarily derived symbioses.

The prediction of pyruvate as the preferred carbon exchange metabolite is controversial. There are a few examples where it is exchanged, for instance it is excreted by the bacterial symbiont of a luminescent fish (Tebo *et al.*, 1979), but these seem to be the

exception. The vast majority of symbioses use simple carbohydrate sources instead: for instance glucose and glycerol are exchanged between dinoflagellates and cnidarians (Burriesci *et al.*, 2012; Muscatine, 1967), maltose between *Paramecium-Chlorella* (Ziesenisz *et al.,* 1981), and malate between Rhizobia-legumes (Prell & Poole, 2006). This may be because pyruvate has a central role in metabolism and is therefore involved in feedback regulation, meaning that changing its concentration could have detrimental knock-on effects (Dinakar *et al.*, 2010; Noguchi & Yoshida, 2008). This is particularly the case in photosynthetic organisms, where glycolysis, the TCA cycle and photosynthesis all regulate one another (Paul & Pellny, 2003). It is noteworthy that in the cases where pyruvate is exchanged, the symbiont is not photosynthetic. The more commonly used simple carbohydrates referred to above are end-products or inputs rather than intermediates and are, therefore, more involved in storage or transport of carbon. Though they may also be involved in 'sink regulation', this would not be detrimental because it is the abundance of carbohydrate end-products, not their depletion, that inhibits photosynthesis (Krapp *et al.*, 1993). It therefore seems likely that a carbohydrate compound and not pyruvate would be exchanged.

This potential regulation constraint for pyruvate cannot be considered by the model because FBA modelling does not include regulation, which can lead to biologically implausible scenarios. Possible regulation conflicts affect many of the intermediates of glycolysis and the TCA cycle. For example, 3-phosphoglycerate has a positive feedback effect on photosystem protein synthesis; therefore, excess depletion could decrease photosynthesis (Takahashi and Murata 2005). These major metabolic pathways have complicated regulation systems that have not even been fully classified, the consequences of which will need to be considered in future research.

The nutrient limitation predictions and the results from the experimental growth of *Synechocystis* on different nitrogen sources both indicate severe carbon limitation. The reason that the growth rate on nitrate is slower than expected could be due to experimental error or it could be, as the limitation results predict, that under the growth conditions *Synechocystis* is more carbon limited than it is nitrogen limited. This means that the organic carbon within the amino acids is having a disproportionately positive effect on growth. Glutamate, which is by far the best nitrogen source in both experiments, is also the nitrogen source with the highest C:N ratio. The common practise of growing *Synechocystis* in increased CO_2 conditions supports this hypothesis.

The model predicted that growth on different nitrogen samples would be accompanied by significant changes to the metabolic pathways used and this was confirmed by mass spectrometry. These predicted changes imply that if *Synechocystis* is provided with glutamate, as is predicted in the symbiosis, its metabolism would be permanently altered. In particular, glycolysis would flow entirely in reverse towards carbon storage, suggesting that the carbon acquired within glutamate is sufficient to drive the TCA cycle, allowing all the carbon acquired by photosynthesis to be directed to storage. This leads to the unusual event of decoupling the TCA cycle and glycolysis. Furthermore, the TCA cycle is complete, which is possibly a result of glutamate being the input for the cycle and the different entry point needing a complete cycle if all intermediates are to be produced.

In addition, the model predicts a change from glutamate to arginine as the endosymbiosis progresses, and because arginine has the most markedly different metabolism, this reveals that perhaps the metabolic adaptation to mutualism is more extreme than to the initial symbiosis. This more severe metabolic shift would, however, have the advantage of being a transition that could develop over longer, evolutionary timescales, while the initial symbiotic event is an abrupt, ecological event.

In addition, the predictions for nutrient limitation have practical applications. For each nutrient, the conditions under which it would be the limiting factor were identified. This knowledge can be used to predict which nutrient is limiting given a set of experimental conditions, and therefore this factor could be alleviated to increase growth. Furthermore, the later work with the different nitrogen sources found that glutamate enriched media improved growth rate by a factor of 5.8.This large improvement to growth could be used to significantly speed up culture time, with implications for both research labs and industrial applications including biofuels.

Future directions:

- Identify the key components of the mass spectra through MS-MS to allow a direct means of testing the model predictions.
- Test whether the differences in uptake rate are responsible for the disparity between the model and experiments, by assaying the concentration of the nitrogen sources over the growth experiment.
- Perform growth assays across the light gradient and at different phosphate concentrations to test the limitation predictions and provide further validation for the model.
- Test a wider range of carbon sources that are first screened for regulation conflicts.
- Improve the model so that it there are no longer regulation conflicts and increase the involvement of the host

Conclusions

This project created different behavioural states within an FBA model, in the form cooperative versus selfish exchange. By comparing the two states predictions were made about how a symbiont could adapt its metabolism in order to transition to an endosymbiotic life style. The results highlight that conflict is at the centre of metabolic exchange. *Synechocystis* selfishly would 'want' to receive glutamate, but in a symbiosis the host also exerts a 'preference'. In an endosymbiosis such as this one where the symbiont is contained in a host vacuole, it is likely that the host would have the strongest influence over the exchange. The most favourable metabolites change if the exchange is assumed to be optimal for both partners. The model has shown that the metabolic nature of the exchange reaction is determined by the level of cooperation and which partner is in control. The metabolites predicted, for various reasons, may not be those that would occur in the actual endosymbiosis; these limitations of the model need to be addressed in order that the model's predictions can be realistic.

This work has demonstrated how FBA modelling can be applied to evolutionary questions. Parameter values are used that allow the metabolism of *Synechocystis* to be studied over a spectrum of cooperation; this analysis is analogous to the potential changes that the symbiont may undergo as it adapts from a free-living organism to living within a host. These predications are applicable to the primary endosymbiotic event and provide a mechanism by which metabolism of an ancient event can be inferred.

References:

Albers, D., W. Reisser, and W. Wiessner. 1982. "Studies on the Nitrogen Supply of Endosymbiotic Chlorellae in Greem Paramecium Bursaria." *Plant Science Letters* 25 (1): 85–90.

Allahverdiyeva, Y., M. Ermakova, M. Eisenhut, P.Zhang, P. Richaud, M. Hagemann, L.Cournac, and E. Aro. 2011. "Interplay between Flavodiiron Proteins and Photorespiration in Synechocystis Sp. PCC 6803." *Journal of Biological Chemistry* 286 (27): 24007–14.

Ball, S., C.Colleoni, U. Cenci, J. N. Raj, and C. Tirtiaux. 2011. "The Evolution of Glycogen and Starch Metabolism in Eukaryotes Gives Molecular Clues to Understand the Establishment of Plastid Endosymbiosis." *Journal of Experimental Botany* 62 (6): 1775–1801.

Bodył, A., P. Mackiewicz, and J. W. Stiller. 2010. "Comparative Genomic Studies Suggest That the Cyanobacterial Endosymbionts of the Amoeba Paulinella Chromatophora Possess an Import Apparatus for Nuclear-Encoded Proteins." *Plant Biology* 12 (4): 639–49.

Bonen, L., and W. F. Doolittle. 1975. "On the Prokaryotic Nature of Red Algal Chloroplasts." *Proceedings of the National Academy of Sciences* 72 (6): 2310–14.
Bratbak, G., and I. Dundas. 1984. "Bacterial Dry Matter Content and Biomass Estimations." *Applied and Environmental Microbiology* 48 (4): 755–57.

Burriesci, M. S., T. K. Raab, and J. R. Pringle. 2012. "Evidence That Glucose Is the Major Transferred Metabolite in Dinoflagellate–cnidarian Symbiosis." *The Journal of Experimental Biology* 215 (19): 3467–77.

Cavalier-Smith, T. 2013. "Symbiogenesis: Mechanisms, Evolutionary Consequences, and Systematic Implications." *Annual Review of Ecology, Evolution, and Systematics* 44 (1): 145–72.

Dean, A. *et al., Journal of Theoretical Biology*, in preparation

Dinakar, C., A. S. Raghavendra, and K. Padmasree. 2010. "Importance of AOX Pathway in Optimizing Photosynthesis under High Light Stress: Role of Pyruvate and Malate in Activating AOX." *Physiologia Plantarum* 139 (1): 13–26.

Dyall, S. D., M. T. Brown, and P. J. Johnson. 2004. "Ancient Invasions: From Endosymbionts to Organelles." *Science* 304 (5668): 253–57.

Fellbaum, C. R., J. A. Mensah, P. E. Pfeffer, E. T. Kiers, and H. Bücking. 2012. "The Role of Carbon in Fungal Nutrient Uptake and Transport." *Plant Signaling & Behavior* 7 (11): 1509–12.

Finlay, B. J., and G. Uhlig. 1981. "Calorific and Carbon Values of Marine and Freshwater Protozoa." *Helgoländer Meeresuntersuchungen* 34 (4): 401–12.

Fischer, E., and U. Sauer. 2005. "Large-Scale in Vivo Flux Analysis Shows Rigidity and Suboptimal Performance of Bacillus Subtilis Metabolism." *Nature Genetics* 37 (6): 636–40.

Flügge, U, and H W Heldt. 1991. "Metabolite Translocators of the Chloroplast Envelope." *Annual Review of Plant Physiology and Plant Molecular Biology* 42 (1): 129–44.

Harcombe, W. R., N. F. Delaney, N. Leiby, N. Klitgord, and C. J. Marx. 2013. "The Ability of Flux Balance Analysis to Predict Evolution of Central Metabolism Scales with the Initial Distance to the Optimum." *PLoS Comput Biol* 9 (6): e1003091.

Hecky, R. E., P. Campbell, and L. L. Hendzel. 1993. "The Stoichiometry of Carbon, Nitrogen, and Phosphorus in Particulate Matter of Lakes and Oceans." *Limnology and Oceanography* 38 (4): 709–24.

Honegger, R. 1991. "Functional Aspects of the Lichen Symbiosis." *Annual Review of Plant Physiology and Plant Molecular Biology* 42 (1): 553–78.

Hörtnagl, P.H., and R. Sommaruga. 2007. "Photo-Oxidative Stress in Symbiotic and Aposymbiotic Strains of the Ciliate Paramecium Bursaria." *Photochemical & Photobiological Sciences* 6 (8): 842.

Ibarra, R. U., J. S. Edwards, and B. O. Palsson. 2002. "Escherichia Coli K-12 Undergoes Adaptive Evolution to Achieve in Silico Predicted Optimal Growth." *Nature* 420 (6912): 186–89.

Johnson, M. D. 2011. "The Acquisition of Phototrophy: Adaptive Strategies of Hosting Endosymbionts and Organelles." *Photosynthesis Research* 107 (1): 117–32.

Kato, Y., and N. Imamura. 2008a. "Effect of Calcium Ion on Uptake of Amino Acids by Symbiotic Chlorella F36-ZK Isolated from Japanese Paramecium Bursaria." *Plant Science* 174 (1): 88–96.

Kato, Y., and N. Imamura. 2008b. "Effect of Sugars on Amino Acid Transport by Symbiotic Chlorella." *Plant Physiology and Biochemistry* 46 (10): 911–17.

Kato, Y., S. Ueno, and N. Imamura. 2006. "Studies on the Nitrogen Utilization of Endosymbiotic Algae Isolated from Japanese Paramecium Bursaria." *Plant Science* 170 (3): 481–86.

Keeling, P. J. 2013. “The Number, Speed, and Impact of Plastid Endosymbioses in Eukaryotic Evolution.” *Annual Review of Plant Biology* 64: 583–607.

Kim, H. W., R. Vannela, C. Zhou, and B. E. Rittmann. 2011. “Nutrient Acquisition and Limitation for the Photoautotrophic Growth of Synechocystis Sp. PCC6803 as a Renewable Biomass Source.” *Biotechnology and Bioengineering* 108 (2): 277–85.

Knoop, H., M. Gründel, Y. Zilliges, R. Lehmann, S. Hoffmann, W. Lockau, and R. Steuer. 2013. “Flux Balance Analysis of Cyanobacterial Metabolism: The Metabolic Network of Synechocystis Sp. PCC 6803.” *PLoS Comput Biol* 9 (6): e1003081.

Kodama, Y., and M. Fujishima. 2011. “Four Important Cytological Events Needed to establishG Endosymbiosis of Symbiotic Chlorella Sp. to the Alga-Free Paramecium Bursaria.” *Jpn. J. Protozool. Vol* 44 (1): 1.

Kodama, Y., and M. Fujishima. 2012. “Cell Division and Density of Symbiotic Chlorella Variabilis of the Ciliate Paramecium Bursaria Is Controlled by the Host’s Nutritional Conditions during Early Infection Process.” *Environmental Microbiology* 14 (10): 2800–2811.

Krapp, A., B. Hofmann, C. Schäfer, and M. Stitt. 1993. “Regulation of the Expression of rbcS and Other Photosynthetic Genes by Carbohydrates: A Mechanism for the ‘sink Regulation’ of Photosynthesis?.” *The Plant Journal* 3 (6): 817–28.

Lower, S. K. (n.d) Carbonate equilibria in natural waters *A Chem1 Reference Text* Available at: http://www.chem1.com/acad/webtext/virtualtextbook.html (Accessed: 20th May 2015)

Mackiewicz, P., A. Bodył, and P. Gagat. 2011. “Possible Import Routes of Proteins into the Cyanobacterial Endosymbionts/plastids of Paulinella Chromatophora.” *Theory in Biosciences* 131 (1): 1–18.

Marin, B., E. C. M. Nowack, and M. Melkonian. 2005. “A Plastid in the Making: Evidence for a Second Primary Endosymbiosis.” *Protist* 156 (4): 425–32.

Martínez, L., V. Redondas, A. García, and A. Morán. 2011. “Optimization of Growth Operational Conditions for CO2 Biofixation by Native Synechocystis Sp.” *Journal of Chemical Technology & Biotechnology* 86 (5): 681–90.

Milne, C. B., P. Kim, J. A. Eddy, and N. D. Price. 2009. “Accomplishments in Genome-Scale in Silico Modeling for Industrial and Medical Biotechnology.” *Biotechnology Journal* 4 (12): 1653–70.

Miwa, I., N. Fujimori, and M. Tanaka. 1996. “Effects of Symbiotic Chlorella on the Period Length and the Phase Shift of Circadian Rhythms in Paramecium Bursaria.” *European Journal of Protistology* 32: 102–7.

Muscatine, L. 1967. “Glycerol Excretion by Symbiotic Algae from Corals and Tridacna and Its Control by the Host.” *Science (New York, N.Y.)* 156 (3774): 516–19.

Muscatine, L., and J. W. Porter. 1977. “Reef Corals: Mutualistic Symbioses Adapted to Nutrient-Poor Environments.” *BioScience* 27 (7): 454–60.

Niittylä, T., G. Messerli, M. Trevisan, J. Chen, A. M. Smith, and S. C. Zeeman. 2004. “A Previously Unknown Maltose Transporter Essential for Starch Degradation in Leaves.” *Science (New York, N.Y.)* 303 (5654): 87–89.

Nogales, J., S. Gudmundsson, E. M. Knight, B. O. Palsson, and I. Thiele. 2012. “Detailing the Optimality of Photosynthesis in Cyanobacteria through Systems Biology Analysis.” *Proceedings of the National Academy of Sciences* 109 (7): 2678–83.

Noguchi, K., and K. Yoshida. 2008. “Interaction between Photosynthesis and Respiration in Illuminated Leaves.” *Mitochondrion*, Unique aspects of plant mitochondria, 8 (1): 87–99.

Nowack, E. C. M., H. Vogel, M. Groth, A. R. Grossman, M. Melkonian, and G. Glöckner. 2011. “Endosymbiotic Gene Transfer and Transcriptional Regulation of Transferred Genes in Paulinella Chromatophora.” *Molecular Biology and Evolution* 28 (1): 407–22.

Nygaard, P., S. M. Bested, K. A. Andersen, and H. H. Saxild. 2000. “Bacillus Subtilis Guanine Deaminase Is Encoded by the yknA Gene and Is Induced during Growth with Purines as the Nitrogen Source.” *Microbiology (Reading, England)* 146 Pt 12 (December): 3061–69.

Ohkawa, H., N. Hashimoto, S. Furukawa, T. Kadono, and T. Kawano. 2011. “Forced Symbiosis between Synechocystis Spp. PCC 6803 and Apo-Symbiotic Paramecium Bursaria as an Experimental Model for Evolutionary Emergence of Primitive Photosynthetic Eukaryotes.” *Plant Signaling & Behavior* 6 (6): 773–76.

Orth, J. D., I. Thiele, and B. Ø Palsson. 2010. “What Is Flux Balance Analysis?” *Nature Biotechnology* 28 (3): 245–48.

Paul, M. J., and T. K. Pellny. 2003. “Carbon Metabolite Feedback Regulation of Leaf Photosynthesis and Development.” *Journal of Experimental Botany* 54 (382): 539–47.

Pfeffer, P. E., D. D. Douds, G. Bécard, and Y. Shachar-Hill. 1999. “Carbon Uptake and the Metabolism and Transport of Lipids in an Arbuscular Mycorrhiza.” *Plant Physiology* 120 (2): 587–98.

Prell, J., and P. Poole. 2006. “Metabolic Changes of Rhizobia in Legume Nodules.” *Trends in Microbiology* 14 (4): 161–68. doi:10.1016/j.tim.2006.02.005.

Ramsey, J. S., S. J. MacDonald, G. Jander, A. Nakabachi, G. H. Thomas, and A. E. Douglas. 2010. “Genomic Evidence for Complementary Purine Metabolism in the Pea Aphid, Acyrthosiphon Pisum, and Its Symbiotic Bacterium Buchnera Aphidicola.” *Insect Molecular Biology* 19 (March): 241–48.

Redfield, A. C. 1958. “The Biological Control of Chemical Factors in the Environment.” *American Scientist* 46 (3): 230A – 221.

Resendis-Antonio, O., J. L Reed, S. Encarnación, J. Collado-Vides, and B. Ø Palsson. 2007. “Metabolic Reconstruction and Modeling of Nitrogen Fixation in Rhizobium Etli.” *PLoS Comput Biol* 3 (10): e192.

Sagan, L. 1967. “On the Origin of Mitosing Cells.” *Journal of Theoretical Biology* 14 (3): 255–74.

Sasaki, T., and H. Ishikawa. 1995. “Production of Essential Amino Acids from Glutamate by Mycetocyte Symbionts of the Pea Aphid, Acyrthosiphon Pisum.” *Journal of Insect Physiology* 41 (1): 41–46.

Schwarz, Zs., and H. Kössel. 1980. “The Primary Structure of 16S rDNA from Zea Mays Chloroplast Is Homologous to E. Coli 16S rRNA.” *Nature* 283 (February): 739–42.

Shah, N., and P. J. Syrett. 1984. “The Uptake of Guanine and Hypoxanthine by Marine Microalgae.” *Journal of the Marine Biological Association of the United Kingdom* 64 (03): 545–56.

Shastri, A. A., and J. A. Morgan. 2005. “Flux Balance Analysis of Photoautotrophic Metabolism.” *Biotechnology Progress* 21 (6): 1617–26.

Silvester, W. B., R. Parsons, and P.W. Watt. 1996. “Direct Measurement of Release and Assimilation of Ammonia in the Gunnera–Nostoc Symbiosis.” *New Phytologist* 132 (4): 617–25.

Small, D. P., R. S. Bennett, and C. D. Bishop. 2014. “The Roles of Oxygen and Ammonia in the Symbiotic Relationship between the Spotted Salamander Ambystoma Maculatum and the Green Alga Oophila Amblystomatis during Embryonic Development.” *Symbiosis* 64 (1): 1–10.

Soldo, A. T., G. A. Godoy, and F. Larin. 1978. “Purine-Excretory Nature of Refractile Bodies in the Marine Ciliate Parauronema Acutum*.” *The Journal of Protozoology* 25 (3): 416–18.

Solomon, C. M., J. L. Collier, G. M. Berg, and P. M. Glibert. 2010. “Role of Urea in Microbial Metabolism in Aquatic Systems: A Biochemical and Molecular Review.” *Aquatic Microbial Ecology* 59 (1): 67–88.

Takahashi, S., and N. Murata. 2006. “Glycerate-3-Phosphate, Produced by CO2 Fixation in the Calvin Cycle, Is Critical for the Synthesis of the D1 Protein of Photosystem II.” *Biochimica et Biophysica Acta (BBA) - Bioenergetics* 1757 (3): 198–205.

Tebo, B.M., D. S. Linthicum, and K. H. Nealson. 1979. “Luminous Bacteria and Light Emitting Fish: Ultrastructure of the Symbiosis.” *Biosystems* 11 (4): 269–80.

Thiele, I., and B. Ø. Palsson. 2010. “A Protocol for Generating a High-Quality Genome-Scale Metabolic Reconstruction.” *Nature Protocols* 5 (1): 93–121.

Thomas, G.H., J. Zucker, S. J. Macdonald, A. Sorokin, I. Goryanin, and A. E. Douglas. 2009. “A Fragile Metabolic Network Adapted for Cooperation in the Symbiotic Bacterium Buchnera Aphidicola.” *BMC Systems Biology* 3: 24.

Tsuchida, T., R. Koga, M. Horikawa, T. Tsunoda, T. Maoka, S. Matsumoto, J. Simon, and T. Fukatsu. 2010. “Symbiotic Bacterium Modifies Aphid Body Color.” *Science* 330 (6007): 1102–4.

Varma, A., and B. Ø. Palsson. 1994a. “Metabolic Flux Balancing: Basic Concepts, Scientific and Practical Use.” *Nature Biotechnology* 12 (10): 994–98.

Varma, A, and B. Ø. Palsson. 1994b. “Stoichiometric Flux Balance Models Quantitatively Predict Growth and Metabolic by-Product Secretion in Wild-Type Escherichia Coli W3110.” *Applied and Environmental Microbiology* 60 (10): 3724–31.

Vigneron, A., F. Masson, A. Vallier, S. Balmand, M. Rey, C. Vincent-Monégat, E. Aksoy, E. Aubailly-Giraud, A. Zaidman-Rémy, and A. Heddi. 2014. “Insects Recycle Endosymbionts When the Benefit Is over.” *Current Biology: CB* 24 (19): 2267–73.

Wang, H., B. L. Postier, and R. L. Burnap. 2004. “Alterations in Global Patterns of Gene Expression in Synechocystis Sp. PCC 6803 in Response to Inorganic Carbon Limitation and the Inactivation of ndhR, a LysR Family Regulator.” *Journal of Biological Chemistry* 279 (7): 5739–51.

Weber, A. P.M., M. Linka, and D. Bhattacharya. 2006. “Single, Ancient Origin of a Plastid Metabolite Translocator Family in Plantae from an Endomembrane-Derived Ancestor.” *Eukaryotic Cell* 5 (3): 609–12.

Wilson, A. C. C., P. D. Ashton, F. Calevro, H. Charles, S. Colella, G. Febvay, G. Jander, et al. 2010. “Genomic Insight into the Amino Acid Relations of the Pea Aphid, Acyrthosiphon Pisum, with Its Symbiotic Bacterium Buchnera Aphidicola.” *Insect Molecular Biology* 19 (March): 249–58.

Yellowlees, D., T. A.V. Rees, and W. Leggat. 2008. “Metabolic Interactions between Algal Symbionts and Invertebrate Hosts.” *Plant, Cell & Environment* 31 (5): 679–94.

Yoo, S., M. H Spalding, and J. Jane. 2002. “Characterization of Cyanobacterial Glycogen Isolated from the Wild Type and from a Mutant Lacking of Branching Enzyme.” *Carbohydrate Research* 337 (21–23): 2195–2203.

Zhang, S., and D. A. Bryant. 2011. “The Tricarboxylic Acid Cycle in Cyanobacteria.” *Science* 334 (6062): 1551–53.

Zhu, X., S. P. Long, and D. R Ort. 2008. “What Is the Maximum Efficiency with Which Photosynthesis Can Convert Solar Energy into Biomass?” *Current Opinion in Biotechnology*, Food biotechnology / Plant biotechnology, 19 (2): 153–59.

Ziesenisz, E., W. Reisser, and W. Wiessner. 1981. “Evidence of de Novo Synthesis of Maltose Excreted by the Endosymbiotic Chlorella from Paramecium Bursaria.” *Planta* 153 (5): 481–85.